AD_____

Award Number: DAMD17-98-1-8167

TITLE: Characterization of Bc1-2, Bc1-xL, and Bax Pore Formation and Their Role in Apoptosis Regulation

PRINCIPAL INVESTIGATOR: Frank Stenner-Liewen, Ph.D.
Sharon Schendel, Ph.D.
John C. Reed, M.D., Ph.D.

CONTRACTING ORGANIZATION: The Burnham Institute
La Jolla, California 92037

REPORT DATE: January 2002

TYPE OF REPORT: Annual Summary

PREPARED FOR: U.S. Army Medical Research and Materiel Command
Fort Detrick, Maryland 21702-5012

NOTICE

USING GOVERNMENT DRAWINGS, SPECIFICATIONS, OR OTHER DATA INCLUDED IN THIS DOCUMENT FOR ANY PURPOSE OTHER THAN GOVERNMENT PROCUREMENT DOES NOT IN ANY WAY OBLIGATE THE U.S. GOVERNMENT. THE FACT THAT THE GOVERNMENT FORMULATED OR SUPPLIED THE DRAWINGS, SPECIFICATIONS, OR OTHER DATA DOES NOT LICENSE THE HOLDER OR ANY OTHER PERSON OR CORPORATION; OR CONVEY ANY RIGHTS OR PERMISSION TO MANUFACTURE, USE, OR SELL ANY PATENTED INVENTION THAT MAY RELATE TO THEM.

LIMITED RIGHTS LEGEND

Award Number: DAMD17-98-1-8167
Organization: The Burnham Institute

Those portions of the technical data contained in this report marked as limited rights data shall not, without the written permission of the above contractor, be (a) released or disclosed outside the government, (b) used by the Government for manufacture or, in the case of computer software documentation, for preparing the same or similar computer software, or (c) used by a party other than the Government, except that the Government may release or disclose technical data to persons outside the Government, or permit the use of technical data by such persons, if (i) such release, disclosure, or use is necessary for emergency repair or overhaul or (ii) is a release or disclosure of technical data (other than detailed manufacturing or process data) to, or use of such data by, a foreign government that is in the interest of the Government and is required for evaluational or informational purposes, provided in either case that such release, disclosure or use is made subject to a prohibition that the person to whom the data is released or disclosed may not further use, release or disclose such data, and the contractor or subcontractor or subcontractor asserting the restriction is notified of such release, disclosure or use. This legend, together with the indications of the portions of this data which are subject to such limitations, shall be included on any reproduction hereof which includes any part of the portions subject to such limitations.

THIS TECHNICAL REPORT HAS BEEN REVIEWED AND IS APPROVED FOR PUBLICATION.

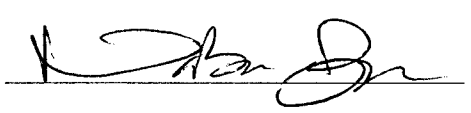

7/22/02

_____ _____

REPORT DOCUMENTATION PAGE

Form Approved
OMB No. 074-0188

1. AGENCY USE ONLY (Leave blank)	2. REPORT DATE	3. REPORT TYPE AND DATES COVERED
	January 2002	Annual Summary (1 Jul 98 - 31 Dec 01)

4. TITLE AND SUBTITLE
Characterization of Bc1-2, Bc1-xL, and Bax Pore Formation and Their Role in Apoptosis Regulation

5. FUNDING NUMBERS
DAMD17-98-1-8167

6. AUTHOR(S)
Frank Stenner-Liewen, Ph.D.
Sharon Schendel, Ph.D.
John C. Reed, M.D., Ph.D.

7. PERFORMING ORGANIZATION NAME(S) AND ADDRESS(ES)
The Burnham Institute
La Jolla, California 92037

E-Mail: rcornell@burnham.org

8. PERFORMING ORGANIZATION REPORT NUMBER

9. SPONSORING / MONITORING AGENCY NAME(S) AND ADDRESS(ES)
U.S. Army Medical Research and Materiel Command
Fort Detrick, Maryland 21702-5012

10. SPONSORING / MONITORING AGENCY REPORT NUMBER

11. SUPPLEMENTARY NOTES

12a. DISTRIBUTION / AVAILABILITY STATEMENT
Distribution authorized to U.S. Government agencies only (proprietary information, Jan 02). Other requests for this document shall be referred to U.S. Army Medical Research and Materiel Command, 504 Scott Street, Fort Detrick, Maryland 21702-5012.

12b. DISTRIBUTION CODE

13. Abstract ***(Maximum 200 Words)*** *(abstract should contain no proprietary or confidential information)*
Bcl-2-family proteins are central regulators of apoptosis and their expression often becomes deregulated in breast cancers. The biochemical mechanisms by which Bcl-2 family proteins control cell life and death decisions are unknown. Recent evidence that certain Bcl-2 family proteins bear structural similarity to the pore-forming domains of bacterial toxin proteins suggest a function for these apoptosis regulators as ion-channels. Using eletrophysiological techniques, we demonstrated that the cytoprotective protein Bcl-2 and the cell death proteins Bax and Bid possess intrinsic ion-channel activity. A variety of structure-function studies demonstrated that channel formation by the Bcl-2 family proteins is important for some but not all of their bioactivities. This finding suggests novel ways to screen for drug inhibitors of Bcl-2, so that tumor cell resistance to cell death can be overcome and sensitivity to anticancer drugs restored

14. Subject Terms (keywords previously assigned to proposal abstract or terms which apply to this award)
Bcl-2, Bcl-xL, Bax, apoptosis, breast cancer, pore formation

15. NUMBER OF PAGES 31

16. PRICE CODE

17. SECURITY CLASSIFICATION OF REPORT	18. SECURITY CLASSIFICATION OF THIS PAGE	19. SECURITY CLASSIFICATION OF ABSTRACT	20. LIMITATION OF ABSTRACT
Unclassified	Unclassified	Unclassified	Unlimited

TABLE OF CONTENTS PAGE

INTRODUCTION

The Bcl-2 family of proteins, which includes Bcl-2, Bcl-x_L, and Bax, serves as regulators of cellular responses to diverse apoptotic stimuli. Bcl-2 and Bcl-x_L encourage cell survival without increasing the rate of cell proliferation, while Bax promotes cell death. It is the ratio of Bcl-2 and Bcl-x_L to Bax, rather that the absolute concentrations that ultimately determines the cell's fate.

Bcl-2, Bcl-x_L, and Bax are expressed in normal mammary epithelium, but their expression changes in breast cancers. In one study, approximately 1/3 of the patients sampled had reduced levels of Bax, which correlated with poor response to therapy and a decreased time to tumor progression and shorter overall survival. A correlation was also found between reduced Bax levels and a reduced amount of Bcl-2 as well as a tendency for such tumors to exhibit mutations in the p53 tumor suppressor, suggesting a global deregulation of apoptotic control mechanisms. An understanding of the biochemical function of these apoptotic regulatory proteins could lead to the development of novel therapies for the treatment of breast cancer.

The amino acid sequences of the Bcl-2 family members have provided few clues as to how these proteins might function biochemically to control apoptosis. The 3-dimensional structure of the soluble form of Bcl-x_L had just been determined when this project was initiated three years ago. Its structure shows a striking resemblance to that of the well-studied membrane-translocation domain of diphtheria toxin and the pore-forming domains of the bactericidal colicins A and E1. The structural similarity between Bcl-x_L and the pore-forming domains of bacterial toxins suggests that the Bcl-2 family of proteins may regulate cell survival through pore formation in organelle membranes. The resulting pores may be able to regulate cell homeostasis by translocation of ions, proteins, or both.

The *in vitro* pore-forming capability of Bcl-x_L and Bcl-2 has been demonstrated both by measurement of channel conductance in planar lipid bilayers demonstrating protein-induced ion efflux from KC1-loaded lipid vesicles. Optimal pore formation occurs at acidic pH, although pores are observable in planar bilayer measurements at neutral pH. The most commonly observed channel conductances of Bcl-x_L and Bcl-2 are ~ 20 and ~ 40 pS, respectively. Both channels prefer cations over anions. The pore-forming activity is highly dependent on the presence of negatively charged lipids. Recently, the channel-forming capability of Bax has been tested on KC1–loaded lipid vesicles. Like Bcl-2 and Bcl-x_L, Bax avidly forms pores at acidic pH.

With the goal of providing insight into the mechanisms of Bcl-2 family proteins, the aims of this project were to address the following questions: (1) what is the nature of the structural changes that must occur to convert Bcl-2 and Bax from soluble to membrane-inserted proteins; (2) which regions of Bcl-2 and Bax participate in pore formation; (3) what is the character of residues lining the channel lumen and what are the relative sizes of the pores formed by Bcl-2 and Bax?

To attain these goals, we utilized membrane-protein biochemistry, assaying Bcl-2 and Bax action on liposome vesicles and planar bilayers. Site-directed mutagenesis was also used, creating Bcl-2-Bax hybrid proteins. We also used biophysical techniques, including circular dichroism and fluorescence spectroscopy of Bcl-2 in the presence of vesicles doped with fluorescence-quenching moieties, and generated cysteine mutants for EPR spectroscopy studies.

BODY

OBJECTIVES:

The originally proposed objectives were partially accomplished:

1. Analyze structural changes accompanying Bcl-2, Bcl-x_L, and Bax membrane insertion.
2. Analyze regions of Bcl-2, Bcl-x_L, and Bax involved in pore-formation.
3. Characterize the pore diameter of Bcl-2 family proteins.

PROGRESS:

TECHNICAL OBJECTIVE #1

Analyze the structural changes accompanying membrane insertion by Bcl-2, Bcl-x_L, and Bax.

Task #1: Lipid binding assays.

This task was accomplished. The optimal lipid composition of membranes for pore-formation by Bcl-2, Bcl-x_L, Bax, and Bid was determined. Acidic phospholipids such as phosphatidyl serine (PS) were found to be required. Neutral lipids such as phosphatidyl choline (PE) did not support protein insertion and pore-formation. These findings were published in (Schendel, et al., *Proc Natl Acad Sci USA*, 94:5113-5118, 1997; Matsuyama, et al., *J Biol Chem*, 273:30995-31001, 1998; and Schendel, et al., *J Biol Chem*, 274:21932-21936, 1999)

Task #2: Generation of single Tryptophan mutants.

A single tryptophan mutant of Bcl-x_L was generated by PCR-based mutagenesis techniques.

Task #3: Purification of single Tryptophan mutants.

The single Tryptophan mutant of Bcl-x_L was expressed in *E. coli* and purified by affinity chromotography.

Task #4: Analyze fluorescence of single Typtophan mutants.

Fluorescence techniques were used to compare the single Tryptophan mutant of Bcl-x_L in the presence of unilammelar liposomes at neutral and acidic pH conditions that control membrane insertion and pore-formation. The sensitivity of the techniques proved to be inadequate for monitoring changes in the location of the Tryptophan residue in aqueous versus membrane environments.

Task #5: Analysis of circular dichroism (ED) spectra of Bcl-2 and Bax in the presence and absence of membranes.

This task was accomplished. We used CD to contrast the secondary structure of Bcl-2, Bax, and Bid in the presence and absence of membranes at neutral (non-inserted) and acidic (inserted) pH. The α-helicity of these proteins was preserved, indicating that membrane insertion involves a change in tertiary but not secondary structure of Bcl-2 family proteins. These results were published (Xie, et al., *Biochemistry*, 37:6410-6418, 1998; and Schendel, et al., *J Biol Chem*, 274:21932-21936, 1999).

Task #6: Molecular modeling of Bcl-x_L for selection of cysteine residues for mutagensis.

This task was accomplished. 3-dimensional models of Bcl-x_L, Bcl-2, Bax, and Bid were constructed using the Rasmol program.

Task #7: Generation of cysteine mutants of Bcl-x_L.

This task was accomplished. Each of the seven α-helicies of Bcl-x_L was individually mutated to insert a single cysteine. Figure 1 depicts the mutants produced.

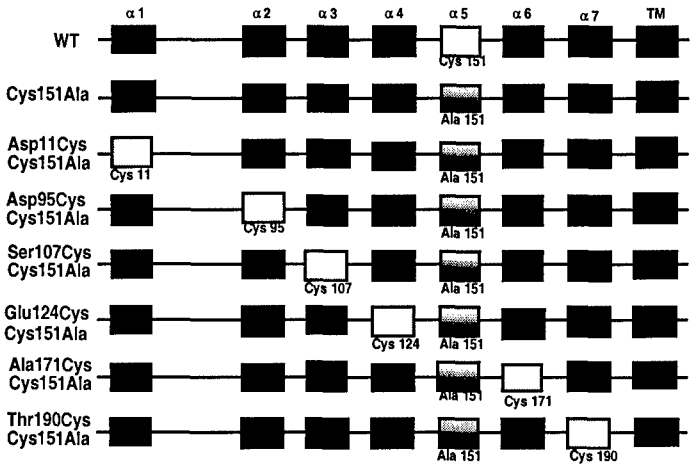

Task #8: Purification of cysteine mutants.

This task was accomplished. The seven mutants of Bcl-x_L were expressed in *E. coli* and affinity purified.

Task #9: Analysis of cysteine mutants.

We conjugated the flourescent compound BODYPI to the sulfhydryl groups of the single cysteine Bcl-x_L mutants. Unfortunately, the BODYPI reagent failed to produce satisfactory results. The dynamic range of the fluorescence changes in BODYPI, with and without addition of anti-BODYPI antibody, was too narrow for producing reliable data. We hope to use these cysteine mutants in the future for alternative approaches to addressing questions about which of the α-helices of Bcl-x_L inserts into membranes.

TECHNICAL OBJECTIVE #2.

Task #1: Assay of Bcl-2 membrane insertion in bromated liposomes.

This task was not addressed.

Task #2: Generation and purification of cysteine mutants for EPR studies.

We delivered the seven cysteine mutants to our collaborator, Wayne Huebbel at UCLA, for EPR analysis. Unfortunately, his laboratory failed to accomplish the EPR analysis. We had no direct access to EPR instrumentation ourselves and thus were unable to accomplish this task

TECHNICAL OBJECTIVE #3.

Task #1: Bcl-2 and Bax mutants devoid of charged residues in hydrophobic core α-helices.

This task was accomplished, we systematically removed polar residues in Bax and then tested the bioactivity of these mutant proteins in both mammalian cells and yeast. We found that polar residues are required for Bax-induced cell death in yeast but not in mammalian (human) cells. In human cells, Bax has two functions; one is related to its pore-forming function; the other is explained by its ability to bind and control the function of other members of the Bcl-2 family. The mutants of Bax that we generated displayed a gain of function phenotype with respect to binding to antiapoptotic protein Bcl-x_L. These findings were published (Nouraini, et al., *Mol Cell Biol*, 20:1604-1615, 2000)

Task #2: Purification of chargeless mutants.

The apolar ("chargeless") mutants of Bax proved to be insoluble when produced in *E. coli*, precluding purification. We attempted multiple alternative methods of expressing these propteins in bacteria, but none were successful.

Task #3: Analysis of chargeless mutants in planar bilayers.

We were unable to analyze the mutants due to protein insolubility. As an alternative, we attempted to express the proteins in Xenopus oocytes and then tried to patch-clamp mitochondria. Some preliminary data were obtained, but the grant expired before we could complete these alternative studies. We hope to return to these experiments when new personnel are available.

Task #4: Optimization of cyt-c encapsulating residues.

This task was accomplished

Task #5: Analysis of Bax and Bcl-2 activity on Cyt-c encapulated residues.

This task was accomplished. In unilamellar liposomes, neither Bcl-2 nor Bax caused release of cytochrome c. These observations are consistent with recent data suggesting that Bax collaborates with either VDAC (Voltage-dependent anion channel) or ANT (Adenine nucleotide translocator) in forming pores that control directly or indirectly the release of cytochrome c. Some of these data were published in collaborative papers with Guido Kroemer's group, (Brenner, et al., *Oncogene* 19:329, 2000).

PUBLICATIONS ATTRIBUTED TO THIS GRANT

A. MANUSCRIPTS:

1. Schendel, S.L., Xie, Z., Montal, M.O., Matsuyama, S., Montal, M. and Reed, J.C.: Channel formation by anti-apoptotic protein, Bcl-2. *Proc Natl Acad Sci USA*, 94:5113-5118, 1997.
2. Schendel SL, Azimov R, Pawlowski K, Godzik A, Kagan BL, Reed JC: Ion-channel activity of the BH3 only Bcl-2 family member, BID. *J. Biol. Chem.*, 274:21932-21936, 1999.
3. Matsuyama, S., Schendel, S.L., Xie, Z.H., Reed, J.C.,: Cytoprotection by Bcl-2 Requires the Pore-Forming α5 and α6 Helices. *J. Biol. Chem.* 273: 30995-31001, 1998.
4. Nouraini, S., Six, E., Matsuyama, S., Krajewski, S., Reed, J.C.: The putative pore-forming domain of Bax regulates mitochondrial localization and interaction with Bcl-X(L). *Mol Cell Biol*, 20:1604-15, 2000.
5. Brenner, C., Cadiou, H., Vieira, H.L., Zamzami, N., Marzo, I., Xie, Z., Leber, B., Andrews, D., Duclohier, H., Reed, J.C., Kroemer, G.: Bcl-2 and Bax regulate the channel activity of the mitochondrial adenine nucleotide translocator. *Oncogene*, 19:329-336, 2000.

B. ABSTRACTS:

1. Xie, Z., Schendel, S.L., Zha, H., Aime-Sempe, C., Matsuyama, S., and Reed, J.C.: pH modulates kinetics of Bcl-2 family protein interactions and their association with membranes. *Blood* 90 (suppl. 1) 52a, 1997.
2. Matsuyama, S., Schendel, S.L., Xie, Z., Reed, J.C.: Cytoprotection by Bcl-2 requires the pore-forming α5 and α6 helices. *Blood* 92 (suppl. 1):373a, 1998.
3. Matsuyama, S., Schendel, S.L., Xie, Z., Reed, J.C.: Cytoprotection by Bcl-2 requires the pore-forming α5 and α6 helices. *Proc. Am. Assc. Cancer Res.* 40:628, 1999.

C. Generated plasmids encoding multiple mutants of Bcl-2, Bcl-x_L, and Bax. Several of these reagents are now available to other scientists at www.sciencereagents.com.

KEY RESEARCH ACCOMPLISHMENTS

1. Demonstrated pore-forming activity of Bcl-2, Bax, and Bid proteins for first time.
2. Demonstrated a role for pore-formation in some but not all aspects of Bcl-2 family function.

REPORTABLE OUTCOMES

1. Published five papers and three abstracts.
2. Generated multiple plasmid reagents which will serve as foundation for future studies.

CONCLUSION

Alterations in the expression of Bcl-2 family proteins occur commonly in breast cancers, including overexpression of anti-apoptotic protein Bcl-2 in ~ 70% and Bcl-x_L in ~ 35% of tumors, as well as loss of Bax expression in ~ 40% of breast cancers. Defects in the expression of Bcl-2 family proteins are sometimes associated with aggressive tumor behaviors, such as poor responses to chemotherapy among breast cancers expressing Bcl-x_L or with loss of Bax expression. Understanding the mechanisms of Bcl-2 family proteins therefore is important if strategies for restoring apoptosis sensitivity to breast cancers are to be realized. The data generated as a result of this grant have contributed to an improved understanding of molecular mechanisms of Bcl-2 family proteins, suggesting novel ways of screening for drugs that might modulate the activities of Bcl-2 family proteins and restore apoptosis competency to breast cancers.

Appendices

Published Work Covered by the Generous Support of DAMD17-98-1-8167

MOLECULAR AND CELLULAR BIOLOGY, Mar. 2000, p. 1604–1615 Vol. 20, No. 5
0270-7306/00/$04.00+0

The Putative Pore-Forming Domain of Bax Regulates Mitochondrial Localization and Interaction with Bcl-X_L

SHAHRZAD NOURAINI, EMMANUELLE SIX,† SHIGEMI MATSUYAMA, STAINSLAW KRAJEWSKI, AND JOHN C. REED*

The Burnham Institute, La Jolla, California 92037

Received 13 September 1999/Returned for modification 21 October 1999/Accepted 29 November 1999

Bax is a proapoptotic member of the Bcl-2 family of proteins which localizes to and uses mitochondria as its major site of action. Bax normally resides in the cytoplasm and translocates to mitochondria in response to apoptotic stimuli, and it promotes apoptosis in two ways: (i) by disrupting mitochondrial membrane barrier function by formation of ion-permeable pores in mitochondrial membranes and (ii) by binding to antiapoptotic Bcl-2 family proteins via its BH3 domain and inhibiting their functions. A hairpin pair of amphipathic α-helices (α5-α6) in Bax has been predicted to participate in membrane insertion and pore formation by Bax. We mutagenized several charged residues in the α5-α6 domain of Bax, changing them to alanine. These substitution mutants of Bax constitutively localized to mitochondria and displayed a gain-of-function phenotype when expressed in mammalian cells. Furthermore, substitution of 8 out of 10 charged residues in the α5-α6 domain of Bax resulted in a loss of cytotoxicity in yeast but a gain-of-function phenotype in mammalian cells. The enhanced function of this Bax mutant was correlated with increased binding to Bcl-X_L, through a BH3-independent mechanism. These observations reveal new functions for the α5-α6 hairpin loop of Bax: (i) regulation of mitochondrial targeting and (ii) modulation of binding to antiapoptotic Bcl-2 proteins.

Members of the Bcl-2 family are major regulators of apoptosis and include both pro- and antiapoptotic proteins. Bax is a proapoptotic Bcl-2 family member which participates in the induction of apoptosis in response to a variety of apoptotic signals (4, 15, 27, 31). Furthermore, overexpression of Bax induces apoptosis in many cells (31, 50). A number of biochemical functions have been defined for Bax, some of which correlate with its proapoptotic activity, including (i) heterodimerization with the proapoptotic Bcl-2 proteins (9, 48, 49), (ii) homodimerization (8, 19, 51), (iii) release of cytochrome *c* from mitochondria (14), and (iv) disruption of the potential across the inner mitochondrial membrane (32, 47). Recently, it has been shown that Bax functionally interacts with components of the mitochondrial inner membrane, the adenine nucleotide transporter (ANT) (22), and the mitochondrial F_0F_1 ATPase H^+ pump (24), as well as the outer membrane voltage-dependent anion channel (VDAC) (40).

The three-dimensional structures of the Bcl-2 family members Bcl-X_L and Bid have been determined, revealing striking resemblance to the pore-forming domains of certain bacterial toxins (2, 25, 35). Moreover, Bcl-2 and Bax can be readily modeled on the same X-ray crystallographic coordinates (36), suggesting that they also possess similar protein folds. This structural homology correlates with the ability of at least four members of the Bcl-2 family, Bcl-X_L, Bcl-2, Bid, and Bax, to form ion-conducting pores in synthetic lipid membranes in vitro (1, 26, 37–39). A hairpin pair of α-helices within the pore-forming domains of bacterial toxins that share structural similarity to Bcl-2 family proteins directly participates in membrane insertion, leading to the generation of voltage-dependent ion-conducting channels (3, 28). Similarly, deletion of the corresponding α-helical hairpin in Bcl-2 and Bax (i.e., α5 and α6) abrogates their ability to form ion-conducting pores in vitro (23, 38), suggesting that this domain performs a similar function in the Bcl-2 family.

The putative pore-forming α-helices in Bcl-2 family proteins are amphipathic. When inserted into membranes, the polar residues of the amphipathic α-helices presumably line the aqueous channels of pores, and this would be expected to play an important role in mediating the function of Bcl-2 family proteins in their capacity as pore-forming proteins. Alternatively, since the α5-α6 domain is involved in membrane insertion, the charged residues within this domain might participate in or regulate interactions of Bax with other proteins within mitochondrial membranes. We therefore generated a series of alanine substitutions for charged residues within the α5 and α6 helices of Bax, evaluating the relevance of these polar residues to the proapoptotic function of the Bax protein.

MATERIALS AND METHODS

Plasmids. Bax mutants were constructed by the method of two-step PCR mutagenesis (10), using a cDNA encoding the open reading frame of mouse Bax (49). The final PCR products were cloned into *Eco*RI and *Xho*I sites of the pSKII plasmid, and the entire mouse Bax open reading frame was sequenced. Subsequently, wild-type (WT) and mutant Bax cDNAs were subcloned into the yeast expression plasmids pGilda (a gift of E. Golemis) and pEMBLGST (a gift of Elain Elion) as *Eco*RI/*Xho*I and *Sma*I/*Hin*dIII fragments, respectively. Bax is expressed as a fusion protein with an N-terminal LexA DNA-binding domain and glutathione-*S*-transferase in the pGilda and pEMBELGST plasmids, respectively. For mammalian expression, the *Eco*RI/*Xho*I fragments of WT and mutant Bax cDNAs were subcloned into the *Eco*RI/*Xho*I and *Eco*RI/*Sal*I sites of HA-pcDNA3 and pEGFP-C2, respectively. Bax is expressed as a fusion protein C-terminal to three contiguous HA tags and to green fluorescent protein (GFP) in HA-pcDNA3 and pEGFP-C2, respectively.

Yeast studies. The yeast strains EGY48 and Brm-1 were used for Bax-mediated cytotoxicity assays (24). Cells were transformed by the lithium acetate method, using 1.0 μg of plasmid DNA and 1.0 μg of sheared, denatured salmon sperm (carrier) DNA. To test viability, transformant colonies were streaked on histidine-deficient (pGilda-based plasmids) or uracil-deficient (pEMBELGST-based plasmids) minimal medium containing either glucose or galactose as a carbon source. The ability of the cells to grow in the presence of Bax expression (on galactose-containing medium) was monitored after incubation at 30°C for 4 to 5 days. For analysis of protein expression, transformants were grown in the appropriate liquid minimal medium containing glucose to an optical density at

* Corresponding author. Mailing address: The Burnham Institute, 10901 N. Torrey Pines Rd., La Jolla, CA 92037. Phone: (858) 646-3140. Fax: (858) 646-3194. E-mail: jreed@burnham-inst.org.

† Present address: Institut Pasteur, URA 1773 CNRS, 75724 Paris Cedex 15, France.

600 nm of 0.4 to 0.5. The cells were washed in H_2O three times before incubation in minimal medium containing galactose for 12 h.

Cell culture, transfection, and mammalian-cell apoptosis assays. Cos-7 and 293T cells were cultured in Dulbecco's modified Eagle's medium supplemented with 10% fetal bovine serum, 1 mM L-glutamine (final concentration), and antibiotics. The transfection reagents Lipofectamine (Gibco BRL) and Superfect (Qiagen) were used for transfection of Cos-7 and 293T cells, respectively. For luciferase-based killing assays, 0.5 μg of either pEGFP-C2 or GFP fusion plasmids, along with 0.1 μg of pGL3 control plasmid (Promega) containing the firefly luciferase gene, was used to transfect 5×10^4 Cos-7 cells in 12-well tissue culture dishes. The transfectants were washed with phosphate-buffered saline and harvested using a luciferase assay system (Promega). Luciferase activity was measured using a luminometer (MicroLumat LB96P; Wallac Inc., Gaithersburg, Md.). To test apoptotic activity in 293T cells, both floating and adherent cells were pooled, fixed in 3.7% paraformaldehyde, and subjected to staining with 4′,6′-diamidino-2-phenylindole (DAPI) 6 to 18 h after transfection with 2.0 μg of pcDNA3 or pEGFP-C2 plasmids encoding WT or mutant Bax. For transfections with pcDNA3 constructs, 0.5 μg of pEGFP-N_2 was included to identify transfected cells. In some transfections, zVAD-fmk (100 μM) was added 2 h after transfection, and apoptotic and cytotoxic activity was assessed by DAPI staining and propidium iodide (PI) dye exclusion, respectively, 48 h posttransfection. To test suppression of Bax activity by Bcl-X_L, 0.5 μg of either WT or mutant GFP fusion plasmids was cotransfected with 1.5 μg of either pcDNA3-Bcl-X_L or pcDNA3 into 293T cells. Cytotoxic and apoptotic assays were performed as described above at 48 h posttransfection.

Confocal microscopy. Cos-7 cells (10^4) in eight-chambered glass slides (LabTek) were transfected with 0.25 μg of either pEGFP-C2 or GFP-Bax (WT or mutant) fusion constructs using 0.75 μl of Lipofectamine. The cells were incubated with or without Staurosporine (STS) (1 μM final concentration) for 4 h, after which they were fixed with 2% paraformaldehyde. To test the localization of Bax in 293T cells, 6×10^5 cells were transfected with 2.0 μg of the above-mentioned plasmids and the cells were harvested 6 h posttransfection, fixed with 2% paraformaldehyde, and mounted on a glass slide. The localization of GFP and GFP fusion proteins was monitored by confocal microscopy using a Bio-Rad laser confocal microscope (MRC-1024).

Immunoblot and immunoprecipitation studies. For immunoblot assays involving yeast, extracts were prepared by breaking the cells using glass beads in lysis buffer (150 mM NaCl, 5 mM EDTA, 50 mM Tris [pH 7.4], 1% NP-40, and protease inhibitors). Aliquots containing 10 μg of total protein were separated in sodium dodecyl sulfate (SDS)–10% polyacrylamide gels, transferred to Immobilon P nylon membranes, and incubated with a polyclonal rabbit anti-LexA antiserum (a gift of E. Golemis). Antigen was detected by incubation of the blots with horseradish peroxidase secondary antibodies followed by the Enhanced ChemiLuminescence detection kit (Amersham). For mammalian expression studies, cells were lysed in radioimmunoprecipitation assay buffer (10 mM Tris [pH 7.4], 150 mM NaCl, 1% Triton X-100, 0.5% deoxycholate, 0.1% SDS, 5 mM EDTA, and protease inhibitors). Aliquots of extracts containing 5 to 30 μg of total protein were analyzed by SDS-polyacrylamide gel electrophoresis immunoblotting as described above. Antigen detection was accomplished using either a polyclonal rabbit anti-mouse Bax (16) or a monoclonal antibody to GFP (Clonetech).

For immunoprecipitation experiments, Cos-7 cells (7.5×10^5/10-mm-diameter dish) were transfected with 5.0 μg of FLAG-Bcl-X_L in pcDNA3 and 5.0 μg of either pEGFP-C2 or GFP fusion Bax plasmids, using 30 μl of Lipofectamine. zVAD-fmk was added to cultures 2 h posttransfection, and the cells were incubated for a further 20 h. Cell extracts were prepared using an isotonic lysis buffer (142.5 mM KCl, 1 mM EGTA, 5 mM $MgCl_2$, 10 mM HEPES [pH 7.4], 0.2% NP-40, and protease inhibitors). Following preclearing of extracts with agarose-GST, Bcl-X_L complexes were immunoprecipitated using an anti-FLAG M2-agarose affinity gel (Sigma). The immune complexes were denatured by boiling them in the presence of Laemmli sample buffer, and aliquots from each sample were loaded into SDS–12% polyacrylamide gels. The presence of Bcl-X_L and GFP-Bax (WT or mutant) complexes was monitored by immunoblotting using a polyclonal anti-human Bcl-X_L (17) and a monoclonal anti-GFP antibody, respectively.

Subcellular fractionation. Cos-7 cells (3×10^6/20-mm-diameter plate) were transfected with 18 μg of HA-pcDNA3 Bax (WT or mutant) along with 2 μg of pEGFP-C2 plasmid, using 60 μl of Lipofectamine. zVAD-fmk (50 μM) was added to the cell cultures 2 h posttransfection, and the cells were incubated for a further 20 h. Then the cells were incubated in the presence or absence of STS (1 μM) for 4 h. Cell extracts were prepared in a hypotonic buffer (5 mM Tris-HCl [pH 7.4], 5 mM KCl, 1.5 mM $MgCl_2$, and protease inhibitors), and fractionated as previously described (43). The heavy-membrane (HM) and light-membrane (LM) fractions were boiled in 100 μl of Laemmli buffer. The soluble fraction was mixed with one-third volume of a 4×-concentrated Laemmli solution and boiled. Aliquots of fractions normalized for cell equivalents were separated on SDS–12% polyacrylamide gels and transferred to Immobilon nylon membranes. Antigen detection was performed using a rat monoclonal antihemagglutinin (anti-HA) high-affinity antibody (Boehringer Mannheim) and a rabbit polyclonal anti-human Bcl-2 antiserum (27). For alkali extractions using HM mitochondrion-enriched fractions, cell extracts were prepared in buffer A (20 mM HEPES [pH 7.4], 10 mM KCl, 1.5 mM $MgCl_2$, 1 mM EDTA, 1 mM dithiothreitol, and protease inhibitors). After a low-speed centrifugation to pellet whole cells and nuclei, the cell extract was divided into two portions, each of which was centrifuged to obtain an HM fraction. One HM fraction was resuspended in a mitochondrial resuspension buffer (120 mM mannitol, 70 mM sucrose, 1 mM EDTA, 1 mM EGTA, and 10 mM HEPES [pH 7.5]). The other HM preparation was resuspended in the same volume of freshly prepared 0.1 M Na_2CO_3 (pH 11.5). Both HM fractions were incubated on ice for 30 min, followed by centrifugation for 10 min at 170,000 × *g* in a Beckman airfuge. Mitochondrial pellets and supernatants were boiled in Laemmli sample solution, normalized for cell equivalents, and separated in SDS–12% polyacrylamide gels. Protein was blotted onto Immobilon-P nylon membranes and probed with a rat monoclonal anti-HA high-affinity antibody (Boehringer Mannheim), a mouse monoclonal antibody to human mitochondrial Hsp60 (Santa Cruz), and a mouse monoclonal antibody (Molecular Probes) recognizing subunit II of human cytochrome *c* oxidase (COX-II).

RESULTS

Cytotoxicity of Bax alanine substitution mutants in yeast. The putative pore-forming α5-α6 region of Bax is predicted to comprise a hairpin-pair of amphipathic α-helices which contains 10 charged residues (Fig. 1). We systematically replaced these charged residues with alanine to investigate their significance for the killing activity of Bax. Bax confers a lethal phenotype when ectopically expressed in the lower eukaryote *Saccharomyces cerevisiae*, with characteristics similar to that imposed by Bax on mammalian cells, including induction of cytochrome *c* release from mitochondria and disruption of mitochondrial membrane potential in a manner that is suppressible by Bcl-2, Bcl-X_L, and Mcl-1 (13, 21, 34, 50). It is highly likely that the ability of Bax to kill yeast is related to its intrinsic activity as a pore-forming protein for two reasons: (i) yeast lacks Bcl-2 family proteins and (ii) deletion of the α5-α6 region of Bax abrogates its lethal effect in yeast (23). As such, yeast provides a convenient readout system for understanding structure-function relations within Bax protein which are relevant to its pore-like activity. Thus, we initially analyzed the cytotoxic activity of the Bax mutants in the yeast *S. cerevisiae* strain EGY48. For these experiments, WT and mutant versions of Bax were expressed in yeast under the control of the *GAL1* promoter, which permits repression and induction of Bax protein expression, by plating cells on media containing glucose or galactose, respectively. As shown in Fig. 2A, the cytotoxic activity of Bax is not compromised upon alanine substitution for up to 7 of 10 charged residues within α5-α6; however, replacement of an additional charged residue (R109), leaving E131 and R147 as the only charged residues, completely abrogated the killing activity of Bax in yeast. Single substitution of tryptophan for the R109 residue did not lead to loss of Bax activity (not shown), suggesting a requirement for multiple substitutions in the putative pore-forming domain for inactivation of the cytotoxic function of Bax in yeast. Measurement of protein expression by immunoblotting (Fig. 2B) showed that the loss of activity of the multiply substituted Bax mutant was not due to instability of the mutant protein.

Neutralization of charged residues in the α5-α6 region of Bax enhances apoptotic and cytotoxic activities. To further evaluate the characteristics of Bax mutants, we first concentrated on Bax mutants B and C, which remain active in yeast and which, among the mutants tested, have the fewest substitutions in the pore-forming domain. Although neutralization of charged residues in the α5-α6 domain did not inactivate the cytotoxicity of Bax in yeast, we considered the possibility that some of these residues in the α5-α6 helix might be required for apoptosis in mammalian cells. For this reason, the apoptotic activity of Bax mutants B (K119A and K123A) and C (K119A, K123A, D142A, R145A, and E146A) was compared with WT Bax in transient-transfection assays in 293T and Cos-7 cells. The Bax B and C mutants induced higher percentages of ap-

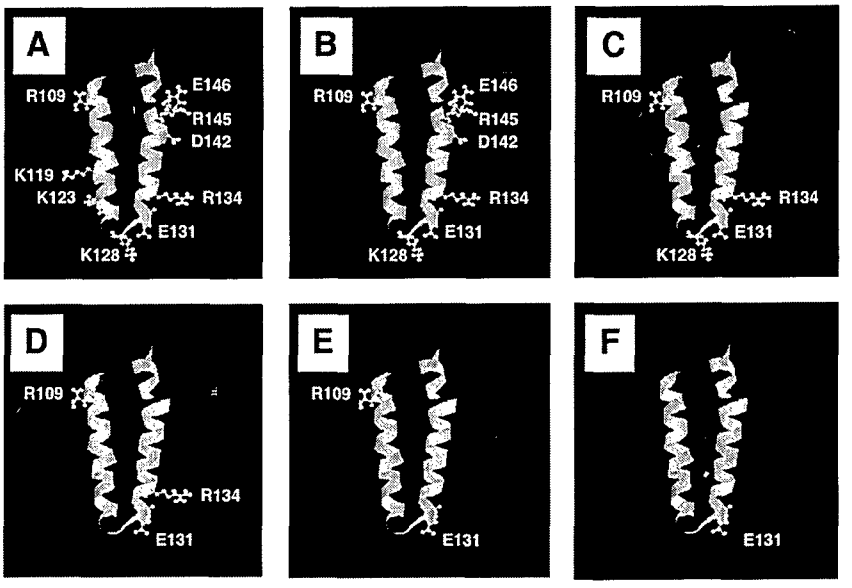

α5 Loop

```
A 106- N W G R V V A L F Y F A S K L V L K A L C T K V P E -131
B      - - - - - - - - - - - - - A - - - A - - - - - - - -
C      - - - - - - - - - - - - - A - - - A - - - - - - - -
D      - - - - - - - - - - - - - A - - - A - - - - A - - -
E      - - - - - - - - - - - - - A - - - A - - - - A - - -
F      - - - A - - - - - - - - - A - - - A - - - - A - - -
```

α6

```
A 132- L I R T I M G W T L D F L R E R L L V W I Q -153
B      - - - - - - - - - - - - - - - - - - - - - - -
C      - - - - - - - - - - A - - A A - - - - - - -
D      - - - - - - - - - - A - - A A - - - - - - -
E      - - A - - - - - - - A - - A A - - - - - - -
F      - - A - - - - - - - A - - A A - - - - - - -
```

FIG. 1. Diagram of mutations generated in Bax. (Top) Ribbon diagrams of the α5-α6 helical hairpin of Bax. The hypothetical three-dimensional structure of Bax was modeled, based on the coordinates available for Bcl-X_L, using the Quanta software package (Molecular Simulations, San Diego, Calif.). The charged residues lining the helical hairpin (residues N106 to Q153) are shown as ball-and-stick representations for WT Bax (A). To illustrate the mutagenic alterations (B to F), the ball-and-stick representations for the residues replaced by alanine are omitted. (Bottom) Amino acid sequence of the α5-α6 regions of WT and mutant Bax proteins. Although the α5-α6 region contains a total of 10 charged residues, we have not considered R147, since it is present in the opposite side of all other charged residues. Accordingly, the ball-and-stick representation of this residue is not depicted in the ribbon diagrams above. The letters on the left correspond to the panels above. The dashes represent residues identical to those in sequence A.

optosis in 293T cells than did WT Bax (Fig. 3A). Similarly, the B and C mutants of Bax were more potent than WT Bax at inducing cell death in Cos-7 cells (Fig. 3B) when tested in a cytotoxicity assay that uses luciferase activity as an endpoint for determining relative numbers of surviving cells (45). Comparison of the steady-state levels of WT and mutant Bax proteins by immunoblot analysis of lysates prepared from 293T and Cos-7 transfectants revealed that the B and C mutant Bax proteins were generally present at slightly lower levels than WT Bax, excluding excessive production of mutants as an explanation for their apparent gain-of-function phenotypes.

To investigate whether the increase in apoptotic activity of Bax mutants is also manifested in yeast, we tested the killing activity of the B and C Bax mutants in the yeast strain Brm-1 (for Bax-resistant mutant 1), which, as we have shown previously, is resistant to the cytotoxic activity of WT Bax (24). In contrast to WT Bax, which was unable to kill the Brm-1 yeast strain, the gain-of-function Bax mutants were cytotoxic, preventing the growth of Brm-1 cells on galactose-containing medium, which induces production of these proteins (Fig. 3C). Immunoblot analysis suggested that the enhanced activity of the B and C Bax mutants was not due to higher levels of

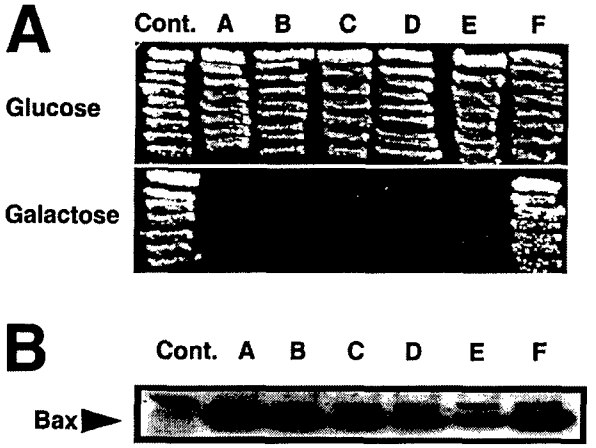

FIG. 2. Cytotoxic activity and expression of Bax mutants in yeast. (A) Yeast strain EGY48 was transformed with 1.0 μg of either the empty yeast expression vector pGilda (Cont.) or pGilda containing WT Bax or the various Bax alanine substitution mutants (the letters correspond to those in Fig. 1). Individual transformant colonies were streaked on histidine-deficient (His^-) medium containing glucose (Bax expression repressed) or His^--galactose (Bax expression induced) semisolid medium and incubated at 30°C for 4 days. (B) Immunoblot results are shown for lysates (10 μg) of yeast cells grown in His^--galactose medium for 12 h. The blot was incubated with anti-LexA antiserum, followed by enhanced chemiluminescence-based detection.

protein production than WT Bax (not shown). We concluded, therefore, that the B and C mutants of Bax display a gain-of-function phenotype in both mammalian cells and yeast.

Cytotoxic activity of gain-of-function mutants of Bax is nullified by Bcl-X_L but not by the caspase inhibitor zVAD-fmk. It has been shown that the cytotoxic activity of Bax arises from two separable components which are caspase dependent and independent (14, 47, 50), with the latter ascribed to the intrinsic function of Bax as a pore-forming protein (reviewed in references 7 and 33). The intrinsic caspase-independent activity of Bax can be monitored by culturing Bax-overexpressing cells in the presence of the broad-spectrum caspase inhibitor zVAD-fmk. Accordingly, 293T cells were transiently transfected with plasmids encoding WT or mutant Bax proteins and then cultured in the presence or absence of zVAD-fmk. The percentages of apoptotic and dead cells were measured after 48 h by DAPI staining and by PI dye exclusion assays, respectively (43, 50). As shown in Fig. 4A, when tested in the absence of zVAD-fmk, WT Bax and the Bax B and C mutants induced both apoptosis and cell death of transiently transfected 293T cells, with the B and C mutants displaying enhanced cytotoxic activity relative to that of WT Bax. In contrast, addition of zVAD-fmk almost completely prevented Bax-induced apoptosis but did not block cell death induction. Moreover, the Bax B and C mutants continued to exhibit enhanced cytotoxic activity relative to WT Bax, even in the presence of zVAD-fmk (Fig. 4). In contrast to zVAD-fmk, which only suppressed Bax-induced apoptosis but not cell death, Bcl-X_L suppressed both apoptosis (nuclear fragmentation as revealed by DAPI staining) and cell death (PI dye uptake) induced by WT and mutant Bax proteins (Fig. 4B). These data argue that the enhanced cytotoxicity of the B and C mutants does not arise through nonspecific mechanisms, since it is suppressible by Bcl-X_L.

Gain-of-function Bax mutants induce apoptosis with accelerated kinetics. To investigate whether the enhanced apoptotic activity of Bax mutants was due to a higher rate of apoptosis induction versus an absolute increase in potency, the time course of apoptosis induction was examined in cultures of 293T cells following transfection with plasmids encoding WT Bax or the B and C mutants of Bax. The GFP-encoding pEGFP-N_2 plasmid was included in all the transfections to monitor transfection efficiency. Although WT Bax induced a lower percentage of transfected cells to undergo apoptosis than did the gain-of-function mutants at 6 h posttransfection, given sufficient time, the apoptotic activity exhibited by WT Bax approached that of the B and C mutants (Fig. 5). Immunoblotting experiments indicated that the faster kinetics of apoptosis induction exhibited by the B and C mutants was not attributable to accelerated production of these proteins in transfected cells compared to WT Bax (Fig. 5, inset). Indeed, WT Bax protein levels were consistently higher than those of Bax-B or Bax-C proteins. This observation suggests that the gain-of-function Bax mutants bypass a rate-limiting step required for Bax protein activation or function.

Bax mutants constitutively localize to mitochondria. Previously, it has been shown that Bax protein resides in the cytosol of some types of cells, undergoing translocation to mitochondrial membranes upon receiving an apoptotic stimulus (11, 12, 46). Since the only early rate-limiting step thus far identified in the Bax pathway for apoptosis is the localization of Bax to mitochondria, we used fluorescence microscopy to monitor the subcellular localization of GFP-tagged WT and mutant Bax proteins. These experiments were performed using Cos-7 cells, in which it has been reported that STS induces the translocation of Bax to mitochondria (11, 12, 46). As shown in Fig. 6A, Bax displayed a uniform distribution in unstimulated Cos-7 cells but localized to cytosolic organellar structures upon treatment with STS. In contrast, the B and C mutants of Bax exhibited a punctate cellular distribution in both the presence and absence of STS (Fig. 6A [only mutant B is shown]). Two-color analysis using a mitochondrion-specific dye (Mitotracker C) confirmed colocalization of Bax to mitochondria following exposure to STS (not shown). We conclude, therefore, that the alanine substitutions in the hyperactive mutants B and C modify the subcellular distribution of these proteins, allowing constitutive mitochondrial localization.

Similar observations were made using 293T cells. In 293T cells, WT Bax constitutively targets mitochondria when overexpressed by transient transfection without the necessity for additional apoptotic stimuli (50). By monitoring GFP-Bax localization in 293T cells at various times after transfection, we observed that WT GFP-Bax was diffusely distributed throughout most cells at 6 h posttransfection (Fig. 6B, left), localizing to mitochondria only in apoptotic cells (Fig. 6B, right). In contrast, the GFP-tagged Bax B and C mutants exhibited a punctate distribution indicative of mitochondrial localization in essentially all cells examined at 6 h posttransfection (Fig. 6B). Cotransfection of Bcl-X_L did not alter the punctate distribution of Bax mutants in 293T or Cos-7 cells (not shown) but did prevent Bax-induced cell death.

To confirm that the punctate distribution of Bax mutants represents constitutive mitochondrial localization, we performed subcellular-fractionation experiments using cell lysates from Cos-7 cells which had been transiently transfected with plasmids encoding HA-tagged WT Bax or Bax mutant B. The cells were cultured in the presence or absence of STS prior to preparation of soluble (cytosolic), LM, and HM fractions. As shown in Fig. 7A, WT Bax was located predominantly in the soluble fractions of unstimulated Cos-7 cells, with a negligible association with membrane fractions in the absence of STS. In contrast, in extracts prepared from STS-treated cells, WT Bax was clearly detected in both the LM and mitochondrion-enriched HM fractions. Although some of the mutant B and C

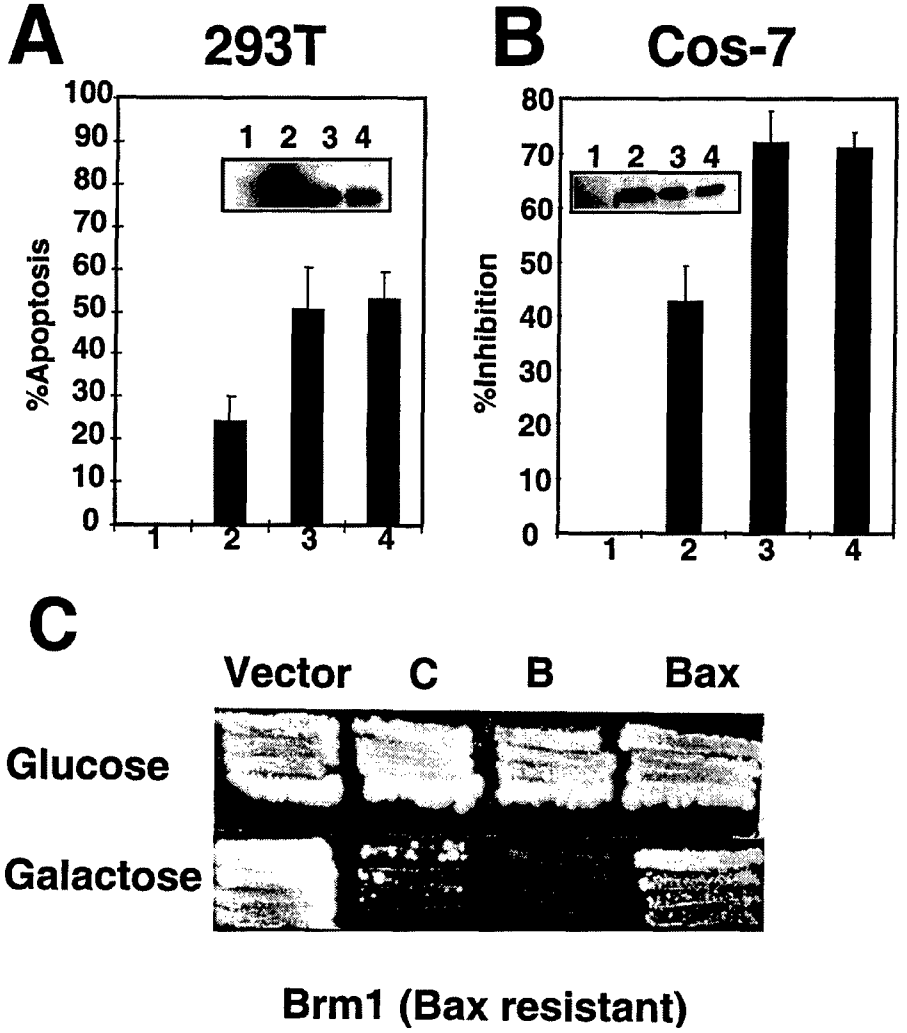

FIG. 3. Bax mutants B and C display a gain-of-function phenotype in mammalian and yeast cells. (A) 293T cells were transfected with empty HA-pcDNA3 vector (bar 1) or pcDNA3 encoding HA-tagged WT Bax (bar 2) or mutant Bax-B (bar 3) or Bax-C (bar 4) protein. The percentage of apoptotic cells (+ standard deviation [SD]) was determined by DAPI staining at 8 h posttransfection. The inset shows an immunoblot analysis of the cells transfected with HA-pCDNA$_3$ (lane 1) or plasmids encoding WT Bax (lane 2) and mutant Bax-B (lane 3) and Bax-C (lane 4), detected with a polyclonal anti-mouse Bax antiserum. (B) Cos-7 cells were transfected with 0.1 μg of the luciferase-encoding plasmid pGL3 control, along with either empty pEGFP-C2 (bar 1), pEGFP-C2–Bax WT (bar 2), pEGFP-C2–Bax mutant B (bar 3), or pEGFP-C2–Bax mutant C (bar 4). The amount of luciferase activity measured for WT and mutant Bax was normalized to that obtained for pEGFP-C2 alone, taking the latter as 100% activity. The results were then subtracted from 100% and plotted as percent inhibition. The data shown represent the averages of three different experiments, each performed in duplicate (mean + SD). The inset shows expression of GFP-WT Bax (lane 2) or GFP-mutant Bax (lanes 3 and 4) proteins detected with a monoclonal antibody to GFP. Lane 1 contains extract from cells transfected with empty vector. (C) The Bax-resistant yeast strain Brm-1 was transformed with 1.0 μg of empty pEMBELGST vector, or pEMBELGST encoding WT Bax or Bax mutants B and C. Transformants were selected on Ura$^-$-glucose$^+$ medium, and individual colonies were grown on Ura$^-$-glucose$^+$ medium (Bax expression repressed) or Ura$^-$-galactose$^+$ medium (Bax expression induced) for 4 days at 4°C.

Bax protein was found in the soluble fraction, a considerable proportion of the Bax-B (Fig. 7A) and Bax-C (not shown) localized to intracellular membranes, including mitochondria, in the absence of STS, unlike WT Bax. These observations thus confirm the results obtained by confocal microscopy using GFP-tagged proteins. Furthermore, the HM-associated Bax-B and Bax-C proteins were mostly membrane inserted, based on their resistance to extraction from membranes by alkali (Fig. 7B and not shown). Examination of soluble (Hsp60) and integral (COX-II) membrane mitochondrial proteins as controls verified successful use of the alkali extraction procedure for assessing the status of WT and mutant Bax proteins (Fig. 7B). We conclude, therefore, that a large fraction of the Bax-B and Bax-C gain-of-function mutant proteins constitutively target and insert in membranes prior to any evidence of apoptosis or stimulation with exogenous apoptosis-inducing agents.

As shown in Fig. 6, mutant Bax-B has a punctate localization throughout the cytoplasm in healthy cells, consistent with the presence of both soluble and membrane-bound Bax-B protein detected in subcellular fractionation experiments (Fig. 7A). However, in apoptotic cells, GFP–Bax-B becomes solely concentrated on mitochondria such that the distributions of mutant and WT Bax become indistinguishable under these conditions (Fig. 6). It has been suggested that in response to apoptotic stimuli, a fraction of soluble Bax localizes to mitochondria and the remaining soluble Bax is removed by prote-

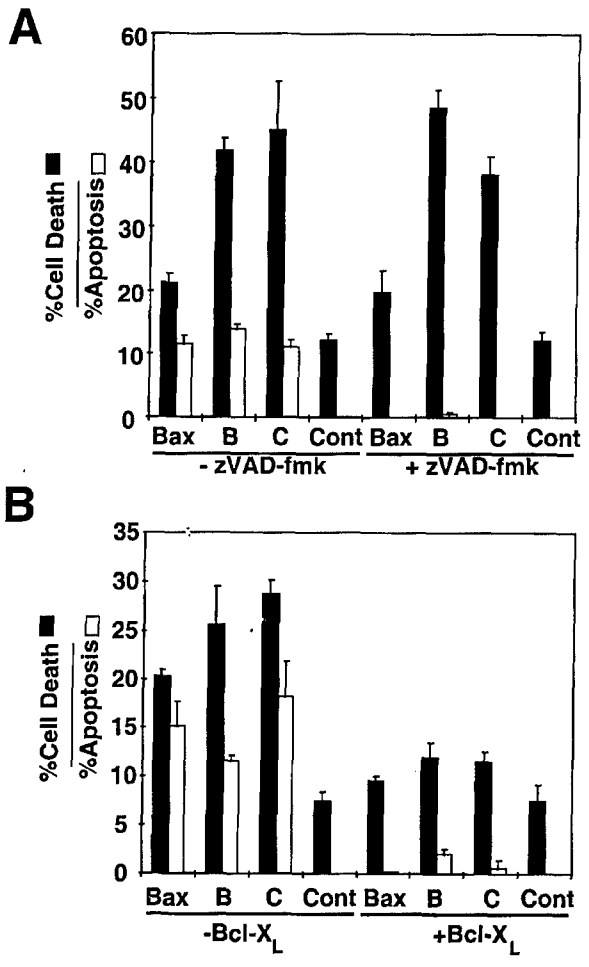

FIG. 4. Inhibition of apoptotic and cytotoxic activity of WT and mutant Bax by zVAD-fmk and Bcl-X_L. (A) zVAD-fmk inhibits the apoptotic but not the cytotoxic activity of WT and mutant Bax. Empty HA-pcDNA3 (Cont) or pcDNA3 encoding HA-WT Bax, Bax-B, or Bax-C (2 μg each) was transfected into 293T cells, followed by culturing in the presence (+) or absence (−) of 100 μM zVAD-fmk. The percentages of apoptotic cells and dead cells were measured by DAPI staining of the nuclei and cellular uptake of PI, respectively, 2 days posttransfection (mean + standard deviation [SD]; $n = 3$). (B) Bcl-X_L inhibits both the apoptotic and cytotoxic activities of WT and mutant Bax. Control HA-pcDNA3 plasmid (Cont) or HA-pcDNA3 plasmids encoding WT Bax or HA-Bax mutants (0.5 μg), were transfected into 293T cells, with or without 1.5 μg of pcDNA3-Bcl-X_L. The cells were scored for apoptotic nuclei and cytotoxic cell death (means + SD) by DAPI staining of nuclei and uptake of PI, respectively, 2 days after transfection.

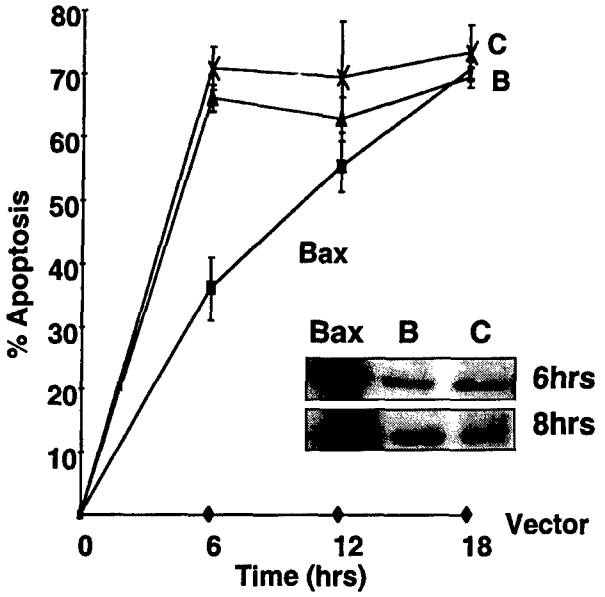

FIG. 5. Gain-of-function Bax mutants kill 293T cells with accelerated kinetics. Plasmid HA-pcDNA3 (Vector) or HA-pcDNA3 encoding WT-Bax (Bax) or mutants Bax-B (B) and Bax-C (C) (2.0 μg each) was transfected into 293T cells. The percentages of apoptotic nuclei were scored 6, 12, and 18 h after transfection (mean ± standard deviation; $n = 3$). The inset is an immunoblot showing the expression of WT and mutant Bax at 6 and 8 h after transfection, using a polyclonal anti-mouse Bax antiserum.

olysis (5). Thus, the difference in the cellular distributions of GFP–Bax-B protein in healthy and apoptotic cells might be due to proteolysis of the fraction of Bax that remains soluble after receipt of an apoptotic signal. Alternatively, the fraction of soluble Bax-B might undergo a conformational change and translocate to mitochondria in apoptotic cells. Nevertheless, the combined data presented in Fig. 6 and 7 indicate that, unlike WT Bax, a large fraction of mutant Bax-B protein constitutively localizes to mitochondria, correlating with a gain-of-function phenotype.

The mutant Bax-F reveals a dual function for the α5-α6 domain. Having evaluated the effects of the Bax mutants (B and C) which contained fewer alanine replacements and which retained cytotoxic activity in yeast, we next turned our attention to the Bax-F mutant, which displayed a loss-of-function phenotype in yeast (Fig. 2) and in which 8 out of 10 charged residues in the α5-α6 domain of Bax had been neutralized. In contrast to the results obtained in yeast, when expressed by transient transfection in 293T and Cos-7 cells, a GFP-tagged Bax-F mutant displayed a gain-of-function phenotype (Fig. 8) and constitutive localization to cellular membranes (not shown). Similar to Bax mutants B and C, Bax-F showed enhanced cytotoxic activity which was suppressed by Bcl-X_L (not shown) but not by zVAD-fmk (Fig. 8C).

Since the cytotoxic activity of Bax in yeast has been attributed to the intrinsic pore-forming activity of Bax, we considered the possibility that the gain-of-function phenotype of Bax mutant F in mammalian cells relates to its ability to bind antiapoptotic Bcl-2 family proteins which are not present in yeast. To test this hypothesis, we made a combination mutant (F+BH3) in which the F mutation was combined with an alanine substitution for the D68 residue in the BH3 domain. Previously, it has been shown that the BH3 domain is the minimal region of Bax required for binding to antiapoptotic Bcl-2 proteins and that a D68A substitution greatly inhibits this interaction (44, 49, 51). The apoptotic activity of the GFP-tagged F+BH3 mutant was compared to that of GFP-tagged WT Bax, Bax-F, and Bax-D68A mutants by transient transfection in 293T and Cos-7 cells.

As shown in Fig. 8, the F+BH3 combination mutant exhibited reduced apoptotic and cytotoxic activity compared to the F mutant in 293T and Cos-7 cells. This reduced activity was not attributable to a change in cellular distribution (not shown) or to impaired production of Bax-(F+BH3) protein, as determined by immunoblot analysis (Fig. 8). However, in both 293T and Cos-7 cells, the F+BH3 mutant retained some killing

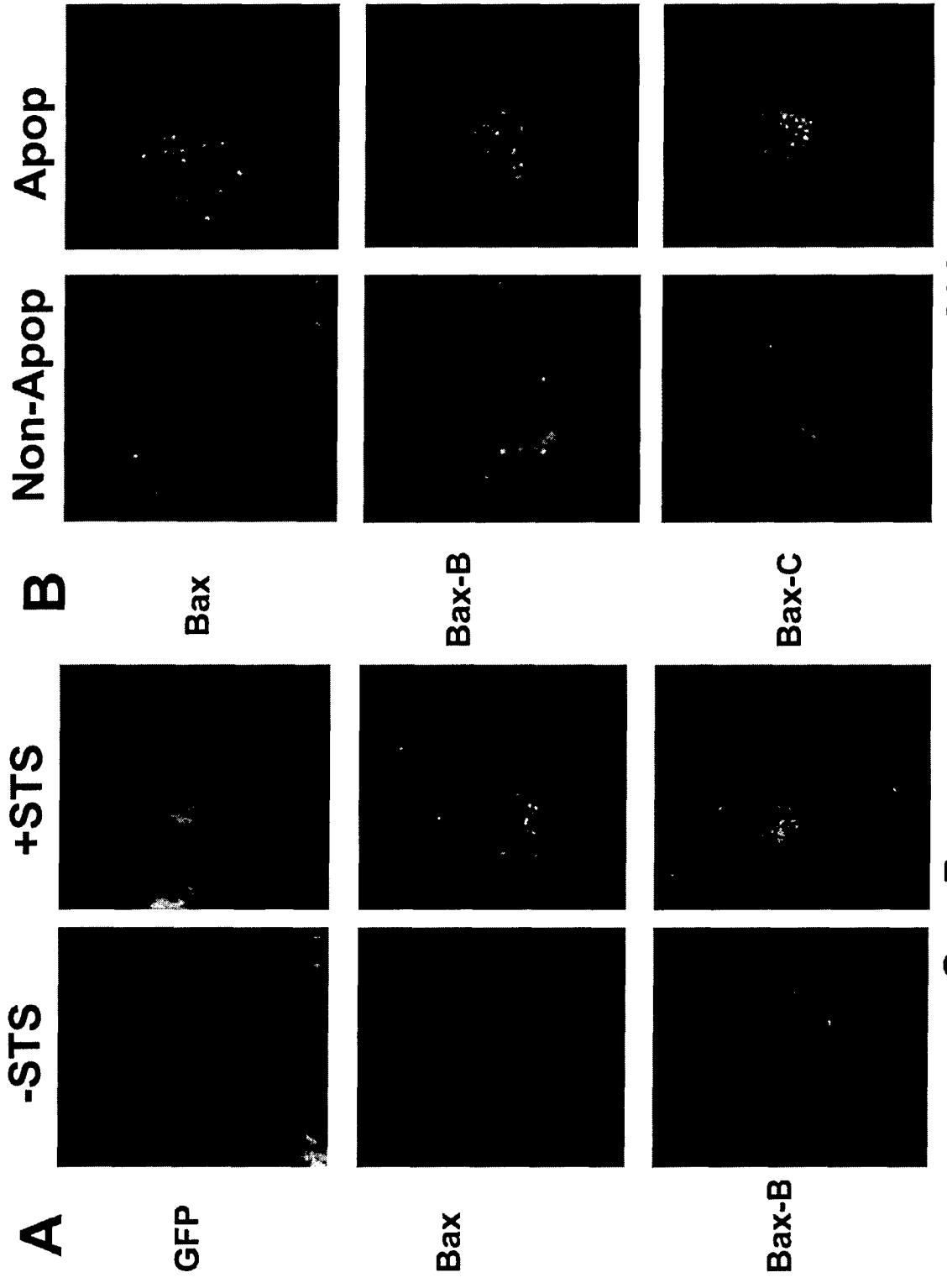

FIG. 6. Bax gain-of-function mutants constitutively localize to cellular membranes. (A) Cos-7 cells were transfected with either pEGFP-C2 or pEGFP-C2 encoding WT Bax or mutant Bax-B. After 20 h of transfection, the cells were incubated with or without STS for 4 h. The cells were fixed, and the localization of GFP and GFP fusion proteins was determined using confocal microscopy. (B) Localization of GFP and various GFP-Bax fusion proteins at 6 h posttransfection in 293T cells. Healthy (non-Apop) and apoptotic (Apop) cells are shown.

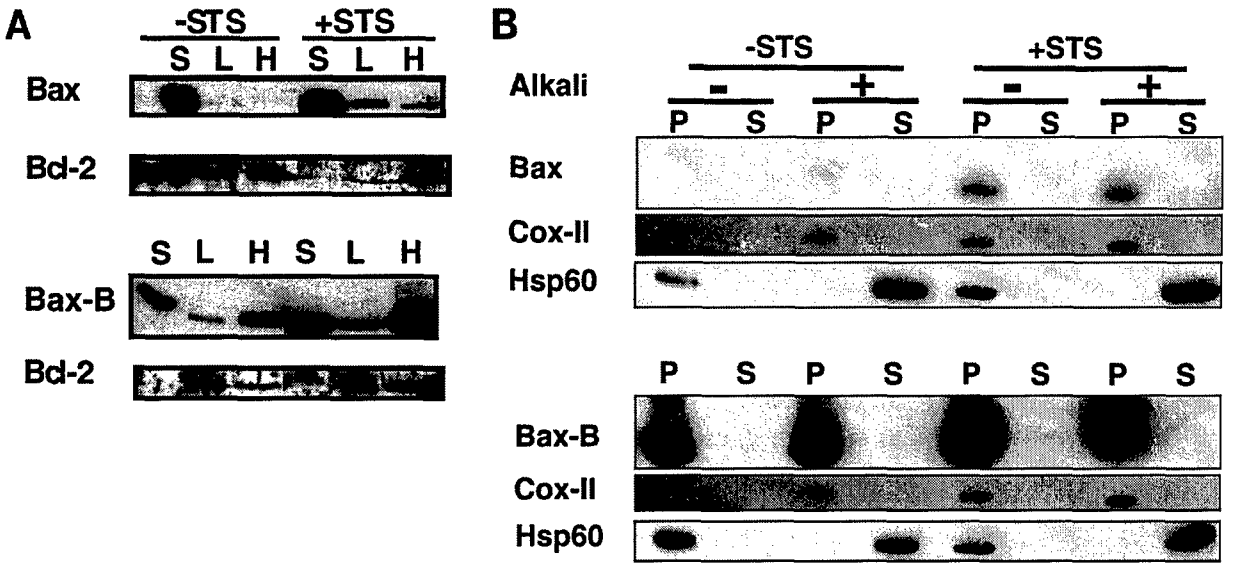

FIG. 7. Analysis of Bax mutants by subcellular fractionation and alkali extraction. Cos-7 cells were transfected with 18 μg of pcDNA3 encoding HA-Bax or HA–Bax-B, followed by incubation for 20 h. Then the transfectants were incubated for 4 h with or without STS. (A) Cell extracts were prepared and fractionated into soluble (S), light-membrane (L), and HM (H) fractions. Aliquots from each fraction normalized to cell equivalents were monitored for the presence of transfected HA-Bax (WT or mutant) and for endogenous Bcl-2 protein by immunoblot analysis using rat monoclonal anti-HA and polyclonal anti-human Bcl-2 antibodies, respectively. (B) Mitochondrion-enriched HM pellets were resuspended in either Na_2CO_3 (pH 11.5) or mitochondrial isolation buffer (pH 7.4). After 30 min of incubation on ice, the mitochondria were pelleted and resuspended in Laemmli sample buffer. Equal proportions of the mitochondrial supernatants (S) and pellets (P) were analyzed by immunoblotting and probing for the presence of HA-Bax (WT or mutant), COX-II (inner membrane), or Hsp60 (matrix or soluble). +, present; −, absent.

activity, despite disruption of its BH3 domain and neutralization of most charged residues in its α5-α6 region.

In an effort to probe the mechanism responsible for the enhanced function of the Bax-F mutant and the residual activity of the Bax-(F+BH3) mutant, we performed coimmunoprecipitation experiments exploring the association of these mutants with Bcl-X_L. For these experiments, Cos-7 cells were transiently transfected with plasmids encoding GFP, GFP-Bax, GFP–Bax-F, GFP–Bax-BH3, or GFP–Bax-(F+BH3), along with FLAG-tagged Bcl-X_L. Immunoprecipitations were then performed with anti-FLAG antibody, and the resulting immune complexes were analyzed for associated Bax protein by SDS-polyacrylamide gel electrophoresis immunoblotting. As shown in Fig. 9, the BH3 domain D68A mutation greatly reduced the interaction of Bax with Bcl-X_L (compare lanes 2 and 3), as previously reported (51). However, when examined in combination with the F mutations, the BH3 domain D68A mutation only partially reduced interaction with Bcl-X_L, compared to WT Bax (Fig. 9, lane 5). Moreover, the Bax mutant F displayed enhanced interaction with Bcl-X_L compared to that of WT Bax (Fig. 9, compare lanes 2 and 4). These observations correlate with the inability of the BH3 domain D68A mutation to completely abolish the apoptotic activity of Bax when combined with the α5-α6 mutant F and provide an explanation for the gain-of-function phenotype of mutant F, despite its lack of cytotoxic activity in yeast.

DISCUSSION

The α5-α6 helical hairpin of Bax has been implicated in the formation of ion-conducting channels in cellular membranes, by analogy to prior work performed with structurally similar bacterial toxins (3, 23). The analogous α-helices of colicins have been shown to insert into membranes, based on electron paramagnetic resonance and fluorescence probe studies (3). Accordingly, the presence of charged residues in the α5-α6 region of Bax imposes certain restrictions on the membrane-inserted state of this protein. One of these is that energetic barriers exist to attaining the membrane-inserted state, since polar residues must be driven into an apolar environment. Second, once inserted into the membrane, the charged residues, residing on one face of each of the amphipathic α-helices in the α5-α6 domain, must be somehow shielded from the lipid bilayer. The most straightforward mechanism for accomplishing this shielding is by directing the polar face of the membrane-inserted α-helices towards the aqueous lumen of a channel and having two or more Bax molecules collaborate by contributing pairs of α-helices that can form a ring around this lumen (reviewed in references 28 and 36). Presumably, this highly charged aqueous lumen would participate in the channel formation and cytotoxicity of Bax by allowing passage of ions through the membrane. We predicted, therefore, that neutralizing charged residues in the α5-α6 region of Bax should make it easier for the protein to attain a membrane-inserted state but also might impair its ability to form ion-permeable cytotoxic channels. The systematic alanine substitutions reported here support these concepts but also reveal previously unidentified functions for the α5-α6 helical hairpin of Bax.

α5-α6 helical hairpin of Bax as regulator of membrane insertion. We have shown that neutralization of as little as two charges in the α5 helix of Bax allows the protein to localize to cellular membranes, including mitochondria. Mitochondria represent a major site of action of Bcl-2 family proteins. Although the antiapoptotic proteins Bcl-2 and Bcl-X_L are predominantly localized to mitochondria and other cellular membranes (46), the proapoptotic protein Bax is normally cytosolic and migrates to the mitochondria in response to undefined apoptotic signals (11, 20, 46). Previous mutational analysis,

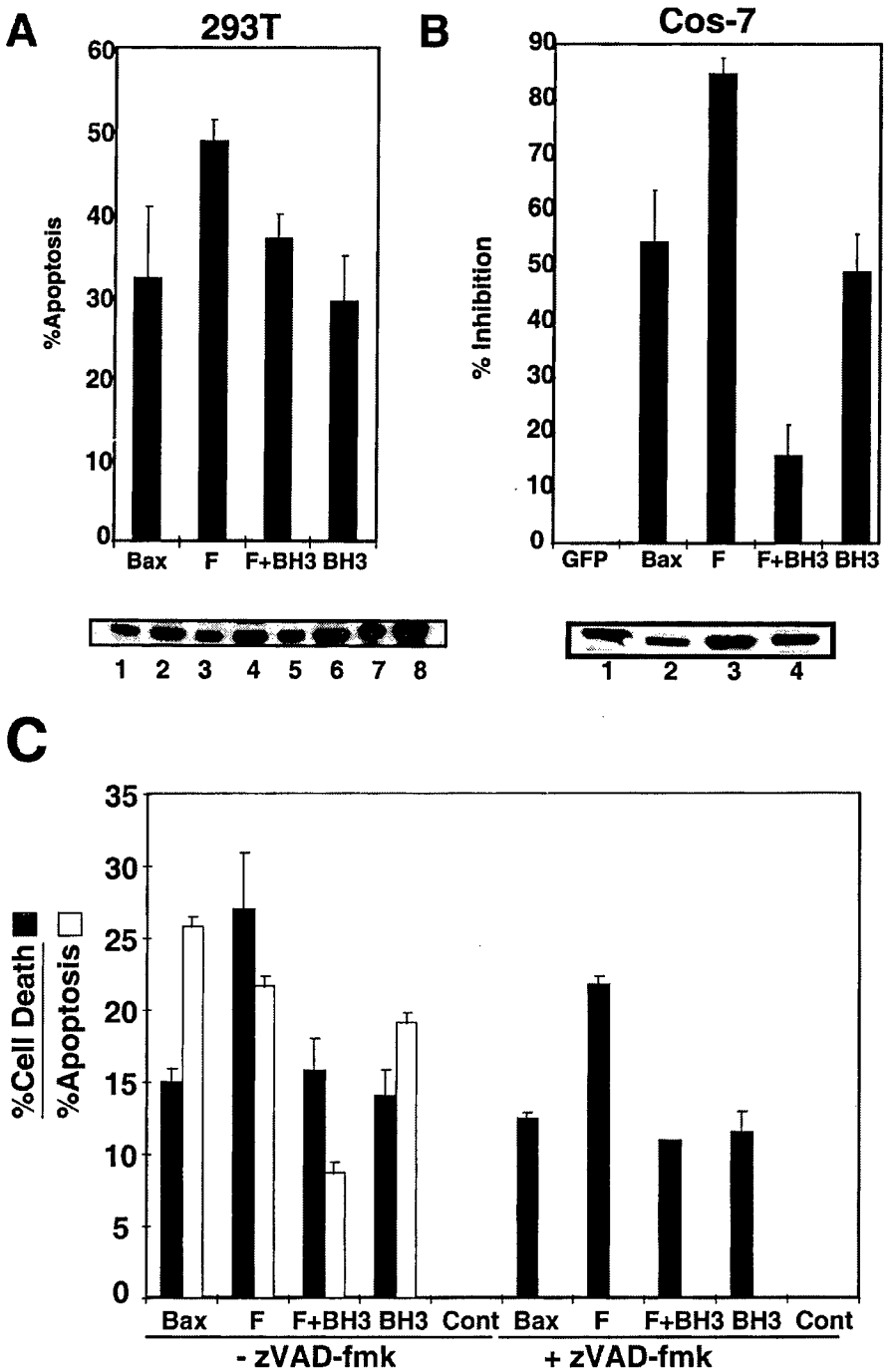

FIG. 8. Apoptotic and cytotoxic activity of Mutant Bax F in mammalian cells. (A and B) Mutant Bax F displays a gain-of-function phenotype in mammalian cells. Plasmids encoding GFP-tagged WT, mutant F, mutant F+BH3, or mutant BH3 (D68A) Bax were transfected into 293T (A) and Cos-7 (B) cells and assayed for apoptosis 5 (A) and 16 (B) h posttransfection, respectively. Protein expression was tested in 293T cells (A, bottom) using either 5 (lanes 1, 3, 5, and 7) or 10 (lanes 2, 4, 6, and 8) μg of protein from extracts of cells transfected with plasmids encoding GFP-Bax (lanes 1 and 2), GFP-F (lanes 3 and 4), GFP-(F+BH3) (lanes 5 and 6), or GFP-BH3 (lanes 7 and 8). For measurement of protein expression in Cos-7 cells (B, bottom), 10 μg of proteins from cells expressing GFP-Bax (lane 1), GFP-F (lane 2), GFP-(F+BH3) (lane 3), or GFP-BH3 (lane 4) was analyzed. Antigen detection for both 293T and Cos-7 extracts was accomplished using monoclonal anti-GFP antibody. (C) zVAD-fmk inhibits the apoptotic, but not the cytotoxic, activity of mutant F. Plasmid DNA was transfected into 293T cells, and zVAD-fmk (100 μM) was added to the cell culture medium 2 h posttransfection. Apoptosis and cytotoxicity were measured by DAPI staining and PI dye exclusion assays, respectively, 48 h posttransfection. The error bars indicate standard deviation. +, present; −, absent.

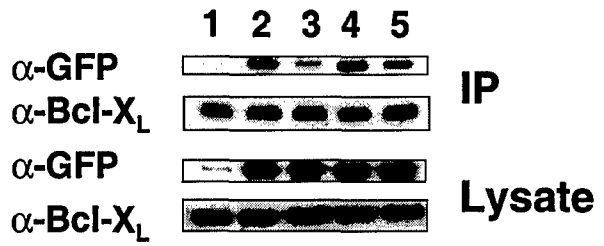

FIG. 9. The gain-of-function phenotype of Bax mutant F correlates with increased binding to Bcl-X_L. Cos-7 cells were transfected with pcDNA3 encoding FLAG-tagged Bcl-X_L, along with plasmids encoding GFP (lane 1) or GFP fusions of WT Bax (lane 2) or Bax mutant F (lane 4), F+BH3 (lane 5), or BH3 (lane 3). Cell extracts were subjected to immunoprecipitation with a monoclonal antibody to the FLAG epitope. The immune complexes and 1/40 of the extract used for coimmunoprecipitations were analyzed by immunoblotting, using a monoclonal antibody to GFP and a polyclonal anti-human Bcl-X_L antiserum. IP, immunoprecipitate.

aimed at determining the regulatory event(s) leading to mitochondrial localization of Bax, have concentrated on the C-terminal hydrophobic domain (TM domain) of this protein (6, 30). The results of these studies suggest that an interaction between the TM domain and the N-terminal first 20 amino acids of Bax prevents Bax from localizing to mitochondria and that a conformational change disrupts this interaction, leading to mitochondrial targeting and membrane insertion (6, 30). The work presented here implicates the charged residues in the α5 helix of Bax as additional determinants of mitochondrial localization. Since the K119A and K123A substitutions in the α5 helix of Bax resulted in mitochondrial localization of a large fraction of mutant B and led to enhanced apoptotic activity, we suggest that either or both of the positively charged residues K119 and K123 are required for maintaining Bax in an aqueous-soluble state. Similar mutational analysis of the membrane insertion α-helical hairpin of diphtheria toxin has shown that substitution of positively charged residues for acidic residues in the loop connecting the two α-helices in this domain (α-helices 8 and 9) blocks membrane insertion (41). This suggests that the presence of positively charged residues is inhibitory for membrane insertion and is consistent with the previously documented energetic unfavorability of inserting positively charged residues into membranes (18). Interestingly, previous studies have shown that enforced dimerization of Bax leads to mitochondrial localization and apoptosis in the absence of external apoptotic stimuli (8, 44). Conceivably, therefore, Bax homodimerization might additionally promote membrane insertion by masking positive charges within the α5-α6 domain.

The α5-α6 helical hairpin as regulator of intrinsic cytotoxic activity of Bax. The cytotoxic activity of Bax in yeast has been attributed to the intrinsic pore-forming capacity of Bax, based on the observation that deletion of the α5-α6 region nullifies the ability of Bax to induce cell death in yeast (23) and due to the absence of Bcl-2 homologues in yeast (reviewed in references 7 and 33). Furthermore, it has recently been shown that Bax functionally interacts with other evolutionarily conserved channel proteins resident in mitochondrial membranes, such as VDAC, ANT, and the F_0F_1 ATPase proton pump, in both yeast and mammalian cells (22, 24, 29, 42). Bax mutants B and C, which largely localize to mitochondria, display gain-of-function phenotypes in both mammalian cells and the Bax-resistant mutant yeast strain Brm-1. Thus, we hypothesize that enhanced membrane insertion facilitates channel formation or interaction with the above-mentioned mitochondrial channel proteins. Since mutant F constitutively localizes to mitochondria but lacks lethal activity in yeast, we predict that this protein is defective in channel activity and/or interaction with other mitochondrial channel proteins. Despite substantial effort, we have been unable to produce any of the Bax mutants as recombinant proteins suitable for direct measurement of channel activity, precluding the determination of the precise biochemical activities that are responsible for the gain-of-function phenotype of mutants B and C and the loss-of-function phenotype of mutant F in yeast.

The α5-α6 region of Bax as a regulator of interactions with Bcl-X_L. Previous studies have suggested that Bax has two mechanisms for killing mammalian cells: one linked to its intrinsic function as a channel-forming or membrane-inserted protein mediated by its α5-α6 region and the other attributable to its ability to dimerize with proapoptotic Bcl-2 family proteins through its BH3 domain, nullifying their cell survival functions (44, 47, 49). Thus, ablating either of these mechanisms individually through mutagenesis of the Bax protein is insufficient to abolish its proapoptotic function in mammalian cells. Despite lacking activity in yeast-killing assays, mutant Bax F, in which 8 of 10 charged residues in α5-α6 were neutralized, displayed a gain-of-function phenotype in mammalian cells. Inasmuch as the Bax-F mutant would be expected to lack intrinsic pore-forming activity, we presumed that the ability of Bax-F to kill mammalian cells but not yeast reflected the BH3-dependent mechanism of killing by Bax. However, when the BH3 domain in Bax-F was mutated (D68A) in a way previously shown to greatly reduce interactions of the WT Bax protein with Bcl-2 and Bcl-X_L (51), the resulting Bax-(F+BH3) mutant protein still retained substantial apoptotic activity. Our attempts to explore the basis for retention of activity by the Bax-(F+BH3) protein have revealed that it retains the ability to associate with Bcl-X_L in coimmunoprecipitation assays. Thus, whereas the BH3 mutation (D68A) greatly reduces binding to Bcl-X_L within the context of the otherwise WT Bax protein (51), it does not prevent association with Bcl-X_L within the context of the Bax-F protein. Moreover, the Bax-F protein displayed enhanced association with Bcl-X_L compared to that of WT Bax, suggesting that alanine substitution neutralization of charged residues in the α5-α6 region of Bax facilitates its interaction with antiapoptotic Bcl-2 family proteins.

The reasons for the apparently enhanced interaction of Bax-F with Bcl-X_L remain to be elucidated. One possibility is that the superior membrane-inserting ability of Bax-F compared to WT Bax allows it to more fully expose the amphipathic face of its BH3 domain, which has been shown to be involved in dimerizing with antiapoptotic Bcl-2 family proteins. Accordingly, perhaps the D68A mutation within the BH3 domain is no longer an impediment to BH3-mediated dimerization in this setting. Alternatively, recent chemical cross-linking studies and other investigations have suggested that membrane-inserted Bax and Bcl-2 or Bcl-X_L may physically interact in membranes in a BH3-independent fashion (44). By favoring membrane insertion, therefore, it is possible that the neutralizing alanine substitution mutations in the α5-α6 region of the Bax-F protein enhance this BH3-independent association of Bax with antiapoptotic proteins, such as Bcl-X_L, affording the protein a gain-of-function phenotype. This putative enhanced interaction of the membrane-inserted forms of Bax and Bcl-X_L hypothetically could abrogate or modify the intrinsic channel activity of the Bcl-X_L protein (44) or could improve the ability of Bax to compete with Bcl-X_L for interactions with other proteins in mitochondrial membranes, such as VDAC or ANT (22, 29, 42). Further investigations are required to distinguish among these possible explanations for the data presented here

and to further delineate the mechanisms of the Bax protein function.

Conclusions. The results reported here support prior suggestions that the Bax protein has a dual mechanism of action: (i) formation of pores in cellular membranes, attributed to the putative pore-forming α5-α6 region, and (ii) heterodimerization with antiapoptotic Bcl-2 family members through the BH3 domain of Bax. Our results, however, also suggest that the α5-α6 domain participates in or regulates interactions of Bax with antiapoptotic Bcl-2 family proteins, such as Bcl-X_L, and that it influences mitochondrial targeting. It remains to be determined whether the α5-α6 domain of Bax participates directly in interaction of the membrane-inserted Bax protein with other integral membrane proteins, such as components of the mitochondrial permeability transition pore complex.

ACKNOWLEDGMENTS

We thank the University of California Tobacco Related Disease Research Program (grant 7FT-0100) and NIH (GM60554) for generous support.

REFERENCES

1. **Antonsson, B., F. Conti, A. Ciavatta, S. Montessuit, S. Lewis, I. Martinou, L. Bernasconi, A. Bernard, J.-J. Mermod, G. Mazzei, K. Maundrell, F. Gambale, R. Sadoul, and J.-C. Martinou.** 1997. Inhibition of Bax channel-forming activity by Bcl-2. Science **277**:370–372.
2. **Chou, J., H. Li, G. Salvesen, J. Yuan, and G. Wagner.** 1999. Solution structure of BID, an intracellular amplifier of apoptotic signaling. Cell **96**:615–624.
3. **Cramer, W. A., J. B. Heymann, S. L. Schendel, B. N. Deriy, F. S. Cohen, P. A. Elkins, and C. V. Stauffacher.** 1995. Structure-function of the channel-forming colicins. Annu. Rev. Biophys. Biomol. Struct. **24**:611–641.
4. **Deckwerth, T. L., J. L. Elliott, C. M. Knudson, E. M. Johnson, Jr., W. D. Snider, and S. J. Korsmeyer.** 1996. BAX is required for neuronal death after trophic factor deprivation and during development. Neuron **17**:401–411.
5. **Desagher, S., A. Osen-Sand, A. Nichols, R. Eskes, S. Montessuit, S. Lauper, K. Maundrell, B. Antonsson, and J.-C. Martinou.** 1998. Bid-induced conformational change of Bax is responsible for mitochondrial cytochrome *c* depletion during apoptosis. J. Cell Biol. **144**:891–901.
6. **Goping, I., A. Gross, J. Lavoie, M. Nguyen, R. Jemmerson, K. Roth, S. Korsmeyer, and G. Shore.** 1998. Regulated targeting of BAX mitochondria. J. Cell Biol. **143**:207–215.
7. **Green, D., and J. Reed.** 1998. Mitochondria and apoptosis. Science **281**: 1309–1312.
8. **Gross, A., J. Jockel, M. Wei, and S. Korsmeyer.** 1998. Enforced dimerization of Bax results in its translocation, mitochondrial dysfunction and apoptosis. EMBO J. **17**:3878–3885.
9. **Han, J., P. Sabbatini, D. Perez, L. Rao, D. Modha, and E. White.** 1996. The E1B 19K protein blocks apoptosis by interacting with and inhibiting the p53-inducible and death-promoting Bax protein. Genes Dev. **10**:461–477.
10. **Ho, S., H. Hunt, R. Horton, J. Pullen, and L. Pease.** 1989. Site-directed mutagenesis by overlap extension using the polymerase chain reaction. Gene **77**:51–59.
11. **Hsu, Y.-T., K. G. Wolter, and R. J. Youle.** 1997. Cytosol-to-membrane redistribution of Bax and Bcl-X_L during apoptosis. Proc. Natl. Acad. Sci. USA **94**:3668–3672.
12. **Hsu, Y. T., and R. J. Youle.** 1997. Nonionic detergents induce dimerization among members of the Bcl-2 family. J. Biol. Chem. **272**:13829–13834.
13. **Jurgensmeier, J., S. Krajewski, R. Armstrong, G. Wilson, T. Oltersdorf, L. Fritz, J. Reed, and S. Ottilie.** 1997. Bax- and Bak-induced cell death in the fission yeast *Schizosaccharomyces pombe*. Mol. Biol. Cell **8**:325–339.
14. **Jurgensmeier, J. M., Z. Xie, Q. Deveraux, L. Ellerby, D. Bredesen, and J. C. Reed.** 1998. Bax directly induces release of cytochrome *c* from isolated mitochondria. Proc. Natl. Acad. Sci. USA **5**:4997–5002.
15. **Knudson, C. M., K. S. K. Tung, W. G. Tourtellotte, G. A. J. Brown, and S. J. Korsmeyer.** 1995. Bax-deficient mice with lymphoid hyperplasia and male germ cell death. Science **270**:96–99.
16. **Krajewski, S., M. Krajewska, A. Shabaik, T. Miyashita, H.-G. Wang, and J. C. Reed.** 1994. Immunohistochemical determination of in vivo distribution of Bax, a dominant inhibitor of Bcl-2. Am. J. Pathol. **145**:1323–1333.
17. **Krajewski, S., M. Krajewska, A. Shabaik, H.-G. Wang, S. Irie, L. Fong, and J. C. Reed.** 1994. Immunohistochemical analysis of in vivo patterns of Bcl-X expression. Cancer Res. **54**:5501–5507.
18. **Krishtalik, L. I., and W. A. Cramer.** 1995. On the physical basis for the *cis*-positive rule describing protein orientation in biological membranes. FEBS Lett. **369**:140–143.
19. **Lewis, S., S. Bethell, S. Patel, J.-C. Martinou, and B. Antonsson.** 1998. Purification and biochemical properties of soluble recombinant human Bax. Protein Expr. Purif. **13**:120–126.
20. **Li, H., H. Zhu, C. Xu, and J. Yuan.** 1998. Cleavage of BID by caspase 8 mediates the mitochondrial damage in the Fas pathway of apoptosis. Cell **94**:491–501.
21. **Manon, S., B. Chaudhuri, and M. Buérin.** 1997. Release of cytochrome *c* and decrease of cytochrome *c* oxidase in Bax-expressing yeast cells, and prevention of these effects by coexpression of Bcl-XL. FEBS Lett. **415**:29–32.
22. **Marzo, I., C. Brenner, N. Zamzami, J. M. Jurgensmeier, S. A. Susin, H. L. A. Vieira, M.-C. Prevost, Z. Xie, S. Matsuyama, J. C. Reed, and G. Kroemer.** 1998. Bax and adenine nucleotide translocator cooperate in the mitochondrial control of apoptosis. Science **281**:2027–2031.
23. **Matsuyama, S., S. Schendel, Z. Xie, and J. Reed.** 1998. Cytoprotection by Bcl-2 requires the pore-forming α5 and α6 helices. J. Biol. Chem. **273**:30995–31001.
24. **Matsuyama, S., Q. Xu, J. Velours, and J. C. Reed.** 1998. The mitochondrial F0F1-ATPase proton pump is required for function of proapoptotic protein Bax in yeast and mammalian cells. Mol. Cell **1**:327–336.
25. **McDonnell, J., D. Fushman, C. Milliman, S. Korsmeyer, and D. Cowburn.** 1999. Solution structure of the proapoptotic molecule BID: a structural basis for apoptotic agonists and antagonists. Cell **96**:625–634.
26. **Minn, A. J., P. Velez, S. L. Schendel, H. Liang, S. W. Muchmore, S. W. Fesik, M. Fill, and C. B. Thompson.** 1997. Bcl-x_L forms an ion channel in synthetic lipid membranes. Nature **385**:353–357.
27. **Miyashita, T., S. Krajewski, M. Krajewska, H. G. Wang, H. K. Lin, B. Hoffman, D. Lieberman, and J. C. Reed.** 1994. Tumor suppressor p53 is a regulator of BCL-2 and BAX in gene expression in vitro and in vivo. Oncogene **9**:1799–1805.
28. **Montal, M.** 1996. Protein folds in channel structure. Curr. Opin. Struct. Biol. **6**:499–510.
29. **Narita, M., S. Shimizu, T. Ito, T. Chittenden, R. J. Lutz, H. Matsuda, and Y. Tsujimoto.** 1998. Bax interacts with the permeability transition pore to induce permeability transition and cytochrome c release in isolated mitochondria. Proc. Natl. Acad. Sci. USA **95**:14681–14686.
30. **Nechushtan, A., C. Smith, Y.-T. Hsu, and R. Youle.** 1999. Conformation of the Bax C-terminus regulates subcellular location and cell death. EMBO J. **18**:2330–2341.
31. **Oltvai, Z., C. Milliman, and S. Korsmeyer.** 1993. Bcl-2 heterodimerizes in vivo with a conserved homolog, Bax, that accelerates programmed cell death. Cell **74**:609–619.
32. **Pastorino, J. G., S. T. Chen, M. Tafani, J. W. Snyder, and J. L. Farber.** 1998. The overexpression of Bax produces cell death upon induction of the mitochondrial permeability transition. J. Biol. Chem. **273**:7770–7775.
33. **Reed, J.** 1998. Bcl-2 family proteins. Oncogene **17**:3225–3236.
34. **Sato, T., M. Hanada, S. Bodrug, S. Irie, N. Iwama, L. H. Boise, C. B. Thompson, E. Golemis, L. Fong, H.-G. Wang, and J. C. Reed.** 1994. Interactions among members of the Bcl-2 protein family analyzed with a yeast two-hybrid system. Proc. Natl. Acad. Sci. USA **91**:9238–9242.
35. **Sattler, M., H. Liang, D. Nettesheim, R. P. Meadows, J. E. Harlan, M. Eberstadt, H. S. Yoon, S. B. Shuker, B. S. Chang, A. J. Minn, C. B. Thompson, and S. W. Fesik.** 1997. Structure of Bcl-xL-Bak peptide complex: recognition between regulators of apoptosis. Science **275**:983–986.
36. **Schendel, S., M. Montal, and J. C. Reed.** 1998. Bcl-2 family proteins as ion-channels. Cell Death Differ. **5**:372–380.
37. **Schendel, S. L., R. Azimov, K. Powlowski, A. Godzik, B. L. Kagan, and J. C. Reed.** 1999. Ion channel activity of the BH_3 only Bcl-2 family member, BID. J. Biol. Chem. **274**:21932–21936.
38. **Schendel, S. L., Z. Xie, M. O. Montal, S. Matsuyama, M. Montal, and J. C. Reed.** 1997. Channel formation by antiapoptotic protein Bcl-2. Proc. Natl. Acad. Sci. USA **94**:5113–5118.
39. **Schlesinger, P., A. Gross, X.-M. Yin, K. Yamamoto, M. Saito, G. Waksman, and S. Korsmeyer.** 1997. Comparison of the ion channel characteristics of proapoptotic BAX and antiapoptotic BCL-2. Proc. Natl. Acad. Sci. USA **94**:11357–11362.
40. **Shimizu, Y., M. Narita, and Y. Tsujimoto.** 1999. Bcl-2 family proteins regulate the release of apoptogenic cytochrome *c* by the mitochondrial channel VDAC. Nature **399**:483–487.
41. **Silverman, J. A., J. A. Mindell, A. Finkelstein, W. H. Shen, and R. J. Collier.** 1994. Mutational analysis of the helical hairpin region of diphtheria toxin transmembrane domain. J. Biol. Chem. **269**:22524–22532.
42. **Vander Heiden, M., N. Chandel, P. Schumacker, and C. Thompson.** 1999. Bcl-X_L prevents cell death following growth factor withdrawal by facilitating mitochondrial ATP/ADP exchange. Mol. Cell **3**:159–167.
43. **Wang, H. G., U. R. Rapp, and J. C. Reed.** 1996. Bcl-2 targets the protein kinase Raf-1 to mitochondria. Cell **87**:629–638.
44. **Wang, K., A. Gross, G. Waksman, and S. J. Korsmeyer.** 1998. Mutagenesis of the BH3 domain of Bax identifies critical residues for dimerization and killing. Mol. Cell. Biol. **18**:6083–6089.
45. **Wang, K., W.-M. Yin, D. T. Chao, C. L. Milliman, and S. J. Korsmeyer.** 1996. BID: a novel BH3 domain-only death agonist. Genes Dev. **10**:2859–2869.
46. **Wolter, K. G., Y. T. Hsu, C. L. Smith, A. Nechushtan, X. G. Xi, and R. J.**

Youle. 1997. Movement of Bax from the cytosol to mitochondria during apoptosis. J. Cell Biol. **139:**1281–1292.

47. **Xiang, J., D. T. Chao, and S. J. Korsmeyer.** 1996. BAX-induced cell death may not require interleukin 1β-converting enzyme-like proteases. Proc. Natl. Acad. Sci. USA **93:**14559–14563.
48. **Yin, X. M., Z. N. Oltvai, and S. J. Korsmeyer.** 1994. BH1 and BH2 domains of Bcl-2 are required for inhibition of apoptosis and heterodimerization with Bax. Nature **369:**321–323.
49. **Zha, H., C. Aime-Sempe, T. Sato, and J. C. Reed.** 1996. Pro-apoptotic protein Bax heterodimerizes with Bcl-2 and homodimerizes with Bax via a novel domain (BH3) distinct from BH1 and BH2. J. Biol. Chem. **271:**7440–7444.
50. **Zha, H., H. Fisk, M. Yaffe, N. Mahajan, B. Herman, and J. Reed.** 1996. Structure-function comparisons of proapoptotic protein Bax in yeast and mammalian cells. Mol. Cell. Biol. **16:**6494–6508.
51. **Zha, H., and J. C. Reed.** 1997. Heterodimerization-independent functions of cell death regulatory proteins Bax and Bcl-2 in yeast and mammalian cells. J. Biol. Chem. **272:**31482–31488.

Oncogene (2000) 19, 329–336

www.nature.com/onc

Bcl-2 and Bax regulate the channel activity of the mitochondrial adenine nucleotide translocator

Catherine Brenner[1,2], Hervé Cadiou[3], Helena LA Vieira[1], Naoufal Zamzami[1], Isabel Marzo[1], Zhihua Xie[4], Brian Leber[5], David Andrews[6], Hervé Duclohier[3], John C Reed[4] and Guido Kroemer*,[1]

[1]*Centre National de la Recherche Scientifique, UPR420, 19 rue Guy Môquet, F-94801 Villejuif, France;* [2]*Centre National de la Recherche Scientifique, UPRES-A6022, Université Technologique de Compiègne, F-60205 Compiègne, France;* [3]*Centre National de la Recherche Scientifique, UMR6522, Université de Rouen (IFRMP 23), F-76821 Mont St. Aignan, France;* [4]*The Burnham Institute, 10901 North Torrey Pines Road, La Jolla, California, CA 92037, USA;* [5]*McMaster University Medical Centre, 1200 Main Street West, Hamilton, Ontario L8N 3Z5, Canada;* [6]*Department of Biochemistry, McMaster University, 1200 Main Street West, Hamilton, Ontario L8N 3Z5, Canada*

Bcl-2 family protein including anti-apoptotic (Bcl-2) or pro-apoptotic (Bax) members can form ion channels when incorporated into synthetic lipid bilayers. This contrasts with the observation that Bcl-2 stabilizes the mitochondrial membrane barrier function and inhibits the permeability transition pore complex (PTPC). Here we provide experimental data which may explain this apparent paradox. Bax and adenine nucleotide translocator (ANT), the most abundant inner mitochondrial membrane protein, can interact in artificial lipid bilayers to yield an efficient composite channel whose electrophysiological properties differ quantitatively and qualitatively from the channels formed by Bax or ANT alone. The formation of this composite channel can be observed in conditions in which Bax protein alone has no detectable channel activity. Cooperative channel formation by Bax and ANT is stimulated by the ANT ligand atractyloside (Atr) but inhibited by ATP, indicating that it depends on the conformation of ANT. In contrast to the combination of Bax and ANT, ANT does not form active channels when incorporated into membranes with Bcl-2. Rather, ANT and Bcl-2 exhibit mutual inhibition of channel formation. Bcl-2 prevents channel formation by Atr-treated ANT and neutralizes the cooperation between Bax and ANT. Our data are compatible with a *ménage à trois* model of mitochondrial apoptosis regulation in which ANT, the likely pore forming protein within the PTPC, interacts with Bax or Bcl-2 which influence its pore forming potential in opposing manners. *Oncogene* (2000) **19,** 329–336.

Keywords: anti-oncogene; mitochondrial transmembrane potential; oncogene; permeability transition; planar lipid bilayer

Introduction

It has recently been recognized that a critical event leading to apoptosis induced in many cell death stimuli involves a change in mitochondrial membrane permeability, culminating in the release of apoptogenic factors such as cytochrome *c*, mitochondrial procaspases, and apoptosis-inducing factor (AIF) from the mitochondrial intermembrane space (Liu *et al.*, 1996; Mancini *et al.*, 1998; Susin *et al.*, 1999b,c; Zamzami *et al.*, 1996). Changes in the flux of ions and water across the inner mitochondrial membrane characterize the early phase of apoptosis, during which an increase in matrix volume may precede a collapse of the inner transmembrane potential ($\Delta\Psi_m$) (Green and Reed, 1998; Kroemer *et al.*, 1998; vander Heiden *et al.*, 1997). These changes are suppressed by Bcl-2/Bcl-X_L, facilitated by Bax, and mediated at least in part by the so-called permeability transition pore complex (PTPC). The PTPC is a two-membrane spanning polyprotein complex containing one of the most abundant inner transmembrane proteins, the adenine nucleotide translocator (ANT, also called ATP/ADP carrier), the most abundant outer membrane protein, voltage-dependent anion channel (VDAC, also called porin), cyclophilin D (a soluble matrix protein), and members of the Bcl-2 family including Bax, Bcl-2 and Bcl-X_L (Crompton *et al.*, 1998; Marzo *et al.*, 1998a,b; Narita *et al.*, 1998; Woodfield *et al.*, 1998). Thus, Bcl-2-like oncoproteins and Bax-like tumour suppressors can interact with sessile mitochondrial proteins involved in the trafficking of intermediate metabolites, in particular in the exchange of ATP and ADP between the matrix and the cytosol (Marzo *et al.*, 1998a,b; Narita *et al.*, 1998).

Bax and Bcl-2 influence the molecular device determining apoptosis resistance or susceptibility (the 'apostat'), at least in part by direct effects on the PTPC (Kroemer, 1997; Marzo *et al.*, 1998a,b; Narita *et al.*, 1998; Shimizu *et al.*, 1998; Zamzami *et al.*, 1996). In isolated mitochondria as well as in purified PTPC reconstituted in liposomes, Bcl-2 can completely prevent the membrane permeabilizing effect of atractyloside (Atr) (Marzo *et al.*, 1998b; Shimizu *et al.*, 1998; Zamzami *et al.*, 1996), a specific ANT ligand whose conformational effects may mimic those mediated by perturbed ADP/ATP gradients (vander Heiden *et al.*, 1997). In contrast, Bax is required for Atr to permeabilize the membranes of purified mitochondria, and recombinant Bax protein can collaborate with purified ANT to create an Atr-responsive channel in artificial membranes (Marzo *et*

*Correspondence: G Kroemer, 19 rue Guy Môquet, B.P. 8, F-94801, Villejuif, France
Received 28 May 1999; revised 15 September 1999; accepted 14 October 1999

al., 1998a). Although proteins from the Bcl-2/Bax family have been originally thought to be confined to the outer membrane, recent data indicate that they are enriched in the inner/outer membrane contact site (where the PTPC is expected to form) (Krajewski *et al.*, 1994) and that they can insert into the inner mitochondrial membrane, in a reaction which depends on the conformation of the ANT/cyclophilin D complex (Marzo *et al.*, 1998a).

Bcl-2, Bcl-X_L, and Bax have been reported to form ion channels when incorporated into artificial membranes (Antonsson *et al.*, 1997; Minn *et al.*, 1997; Schendel *et al.*, 1997; Schlesinger *et al.*, 1997). The channels formed by Bcl-X_L and Bcl-2 have several levels of conductance (80, 130, 180, 280 pS for Bcl-X_L; 20, 40, 90 pS and up to 1.9 nS for Bcl-2) and exhibit mild K^+ selectivity (Minn *et al.*, 1997; Schendel *et al.*, 1997; Schlesinger *et al.*, 1997). In contrast, Bax demonstrates mild Cl^- specificity. Its conductance may raise from values of 26, 80, 180, and 250 pS to maximum levels of 1.5-2 nS (Antonsson *et al.*, 1997; Schlesinger *et al.*, 1997). Purified ANT, which normally is a strict ADP/ATP antiporter, forms channels in response to Ca^{2+} in the range of 300–600 pS (Brustovetsky and Klingenberg, 1996).

How ANT, Bcl-2 and Bax differentially regulate mitochondrial membrane permeabilization in intact organelles (ANT and Bax as facilitators, Bcl-2 as an inhibitor) is unclear, given that they all can act on artificial membranes to increase their permeability. Intrigued by this paradox, we decided to evaluate possible cooperative effects between ANT, Bax and Bcl-2 in artificial membranes, comparing the electrophysiological properties of these proteins in pairwise combinations (ANT-Bax or ANT-Bcl-2) with each of the proteins alone. Our data indicate that Bax increases the capacity of ANT to form active channels with Atr, whereas Bcl-2 reduces channel formation by ANT. These observations may explain the mode of action of Bcl-2 which, in its physiological context, is likely to act as a channel inhibitor rather than as an autonomous ion channel.

Results and discussion

Functional interaction between ANT and mitochondrion-targeted Bcl-2 in intact cells

Bcl-2 prevents the Atr-induced mitochondrial swelling, $\Delta\Psi_m$ dissipation, and release of soluble intermembrane proteins in isolated mitochondria (Susin *et al.*, 1996, 1999b; Zamzami *et al.*, 1996). We have validated this result in intact cells, in which the mitochondrion-targeted expression of Bcl-2 (but not the expression of Bcl-2 in the endoplasmic reticulum) prevents the $\Delta\Psi_m$ collapse and nuclear apoptosis induced by microinjection of Atr (Figure 1a,b). As a control, Bcl-2, however, fails to inhibit manifestations of apoptosis induced by microinjected apoptogenic proteins such as cytochrome *c* (Figure 1b). Collectively, these data confirm and extend our earlier observations suggesting a close functional interaction between the target of Atr, ANT, and proteins from the Bcl-2/Bax family within the PTPC (Marzo *et al.*, 1998a,b).

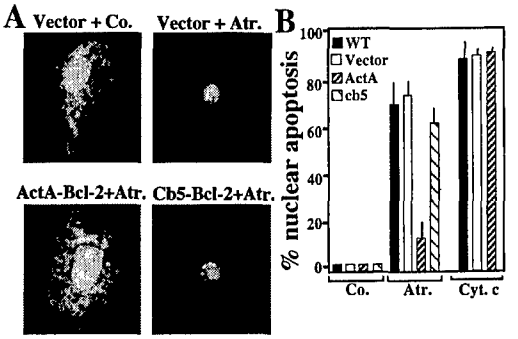

Figure 1 Differential effect of mitochondrial or extramitochondrial Bcl-2 overexpression on apoptosis induced by the ANT ligand Atr. Rat-1 cell transfected with a control vector or cells expressing Bcl-2 either in mitochondria (actA-Bcl-2 fusion protein) or in the endoplasmic reticulum plus nucleus (cb5-Bcl-2 fusion protein) were microinjected with buffer only (control) or Atr. Two hours after microinjection of Atr, cells were stained with the $\Delta\Psi_m$-sensitive dye CMXRos and the DNA-intercalating dye Hoechst 33342. Representative cells are shown on the left and the frequency of cells having undergone nuclear apoptosis after injection of buffer only, Atr, or cytochrome *c* is shown on the right. At least 200 cells were injected for each data point (mean ± s.d., $n=3$)

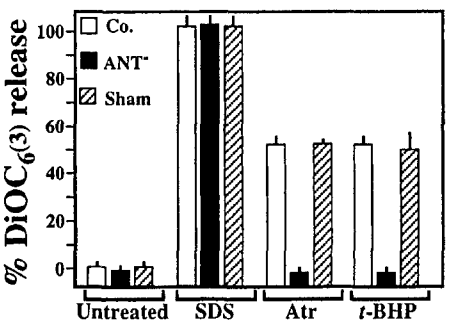

Figure 2 Identification of ANT as a functionally important PTPC constituent. PTPC were either ANT depleted or sham-immunodepleted and reconstituted into liposomes, treated with Atr or *tert*-butylhydroperoxide, and determination of $DiOC_6$ (3) retention within liposomes in the flow cytometer, as described in the Materials and methods section ($n=2$). Incubation of liposomes with SDS marks the 100% value of liposomal membrane permeabilization

ANT is the major Atr target within the PTPC

The semi-purified PTPC can be reconstituted into liposomes and responds to a variety of inducers including Atr or the pro-oxidant *t*-BHP by increasing membrane permeability to small (<1500 Da) solutes such as $DiOC_6$(3). Upon immunodepletion of ANT, the capacity of PTPC to confer Atr- or *t*-BHP-induced membrane permeabilization is abolished, suggesting that ANT is the likely Atr target within the PTPC (Figure 2). Purified ANT, which lacks any immunodetectable contamination by ANT-interacting proteins such as VDAC, cyclophilin D, Bax, or Bcl-2 (Figure 3a), can be reconstituted into planar lipid bilayers. In

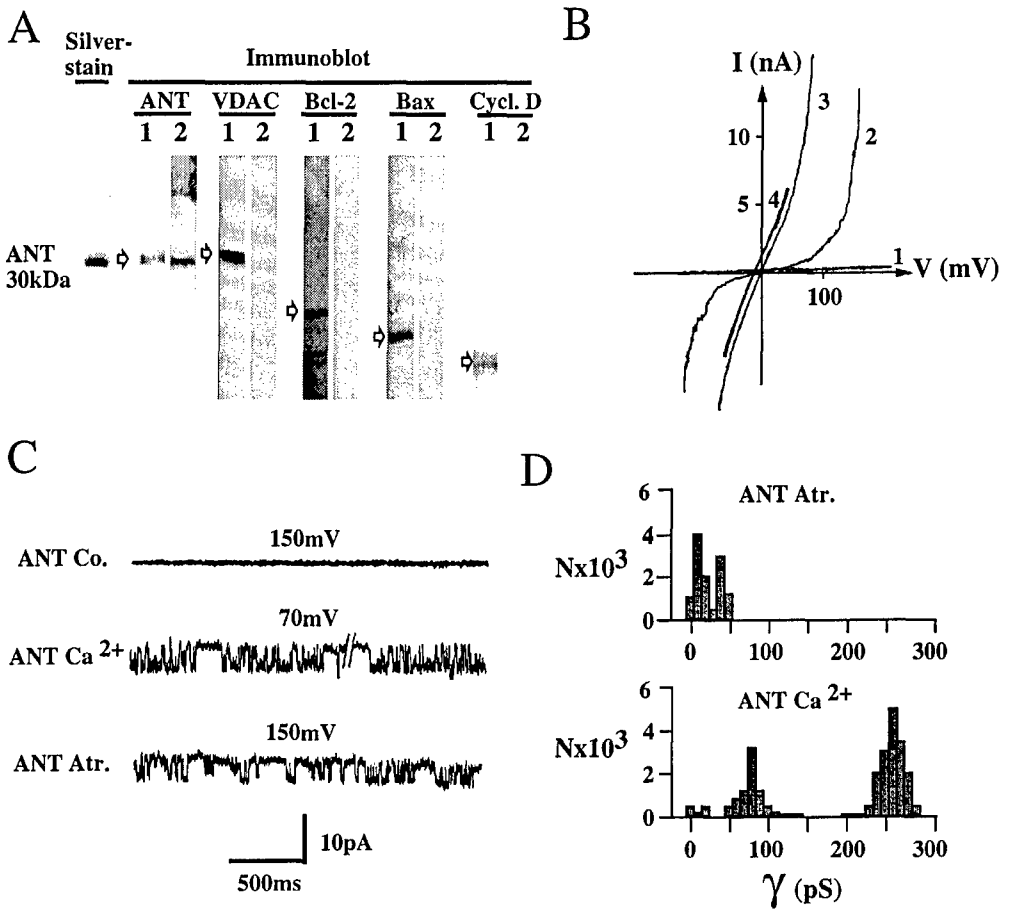

Figure 3 Electrophysiological properties of purified ANT. (**a**) Purification of ANT. Three μg of purified ANT was separated by SDS–PAGE and silver-stained. Immunoblots of 50 μg of proteins from rat heart mitochondria (lane 1) or 3 μg purified ANT were performed for the detection of ANT, Bax, VDAC, and cyclophilin D, as described in Materials and methods (lane 2). As positive control for Bcl-2 immunodetection, mitochondria from the HT 29 cell line were used (lane 1). Arrows indicate the presence of specific bands in positive controls. (**b**) Macroscopic conductance of ANT. ANT was reconstituted into synthetic lipid bilayers, and submitted to slow voltage ramps (1 min/cycle) to determine the current at different voltages in symmetric conditions (100 mM KCl on both sides of the membrane), either in the absence (line 1) or in the presence of 40 μM Atr (line 2) or 1 mM $CaCl_2$ (line 3). The macroscopic conductance of Atr-treated ANT was also recorded in asymmetric conditions (100/400 mM $CaCl_2$ KCl + 1 mM $CaCl_2$, line 4). Results are representative of three independent determinations. (**c**) Single-channel recordings of ANT channels induced by Ca^{2+} or Atr. Recordings were obtained using the dip-tip method (same concentrations of ANT, Atr or $CaCl_2$ as in (**b**) and were representative of the most frequently observed channels. c: closed state; o: open state. (**d**) Statistical analysis of conductances of Atr. and Ca^{2+} induced ANT channels. The conductance levels (γ) observed for single channel openings (obtained as in **c**) were plotted against the frequency (N) of events

accord with previous observations (Brustovetsky and Klingenberg, 1996), ANT has little if any capacity to increase the current on planar lipid bilayers in a voltage-dependent fashion (line 1 in Figure 3b). However, after addition of Atr or Ca^{2+}, ANT mediates significant conductance (lines 2 and 3 in Figure 3b) in macroscopic determinations. Of note, the channel formed by ANT is slightly cation specific under an applied 400/100 mM KCl (cis/trans) gradient, yielding a Vrev of ~ -15 mV (line 4 in Figure 3b) and a P_K:P_{Cl} ratio of 2.8. Single channel recordings obtained at optimal voltages confirm that ANT by itself does not form any channels (Figure 3c), yet forms channels in response to Ca^{2+} with two levels of conductance (70 and 250 pS in Figure 3c,d). In response to Atr, ANT forms only one channel species with a relatively low conductance (30 pS in Figure 3c,d), as compared to Ca^{2+}. In conclusion, ANT is required for the Atr response of PTPC and can, by itself, form an Atr responsive channel.

ANT and Bax cooperate to form an Atr-responsive channel

Single channel recordings reveal that a mixture of Bax and ANT (molar ratio 1 : 4) has a higher probability of pore opening and possesses at 150 mV conductance levels (30 and 80 pS) different from what might be expected from the simple addition of Bax-mediated channels ($\sim$200 pS) to Atr-treated ANT (30 pS, see above, Figure 3d) (Figure 4a,b). Moreover, when employed at relatively low doses (1 nM), Bax does not yield any major macroscopic conductance (line 1 in

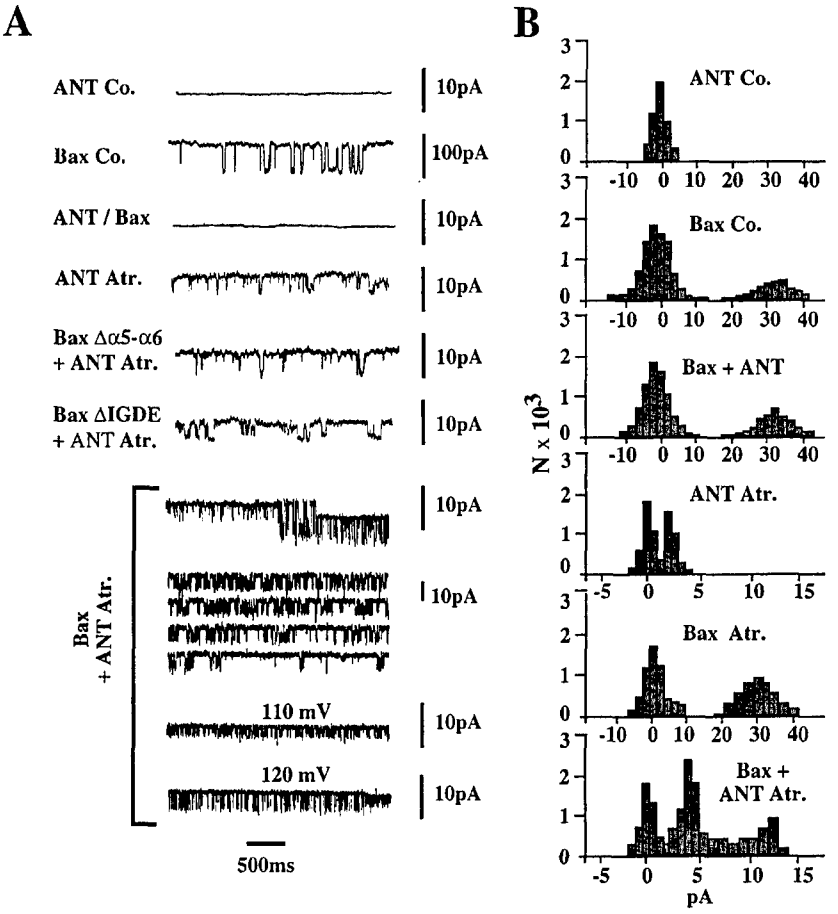

Figure 4 Cooperation between ANT and Bax in tip-dip experiments. (**a**) Cooperative effect at the single channel level. ANT (treated with 40 μM Atr or not) and/or recombinant Bax protein (molar ratio ANT : Bax = 4 : 1) or Bax mutant proteins (Bax $\Delta\alpha$5/6 or Bax ΔIGDE, used at the same ratio as Bax wild-type protein) were incorporated into synthetic membranes and single channel recordings were performed using the dip-tip technique. The applied voltage was 150 mV unless specified differently and the recordings shown are representative for at least three independent determinations. Note that the scale of the ordinate is indicated for each recording. (**b**) Statistical analysis of conductances obtained in (**a**). Results were expressed as current distributions at different voltages. Conductances may be calculated by division of current by voltage

Figure 5a), unless combined with ANT treated with Atr (line 4 in Figure 5a). Thus, the combination of ANT + Atr + Bax (line 4) forms a much more efficient membrane permeabilizing channel than do the combinations ANT + Atr (line 2), ANT + Bax (line 3 in Figure 5a), or Atr + Bax (not shown). The ANT/Bax cooperation is not observed when wild-type Bax is replaced by two mutant proteins which have lost their apoptogenic potential (Matsuyama *et al.*, 1998; Ying *et al.*, 1994): Bax ΔIGDE, which lacks a homodimerization domain in BH3, and Bax $\Delta\alpha$5/6, which lacks a putative pore forming domain (Figure 5b). Preincubation of ANT with its physiological ligand ATP completely inhibits the channel activity mediated by ANT + Atr + Bax (Figure 5b). The channel formed by ANT + Bax is K^+ specific (line 5 in Figure 5a). Thus the combined ANT/Bax channel resembles that formed by ANT (which is also cation-specific, line 4 in Figure 3b), yet differs from that formed by Bax alone (which is anion-specific) (Schendel *et al.*, 1997).

In summary, Bax and ANT can cooperate by forming a new class of channels which acquire distinct electrophysiological properties as well as a far higher probability of opening than either of the two compounds on its own. This cooperative effect depends on the conformation of the ANT, as manifested by the effects of actractyloside and ATP.

Bcl-2 inhibits the formation of an Atr-responsive, ANT-dependent channel

As previously reported (Minn *et al.*, 1997; Schendel *et al.*, 1997; Schlesinger *et al.*, 1997), Bcl-2 can form a channel when incorporated into artificial membranes (Figure 6a). This effect was obtained at neutral pH, provided that Bcl-2 was mixed with dried lipids, prior to generation of the lipid bilayer (Figure 6a,b); it was not observed for a Bcl-2 mutant protein lacking the putative α5/6 membrane insertion domain (Schendel *et al.*, 1997) and was modified by a single amino acid exchange in the BH1

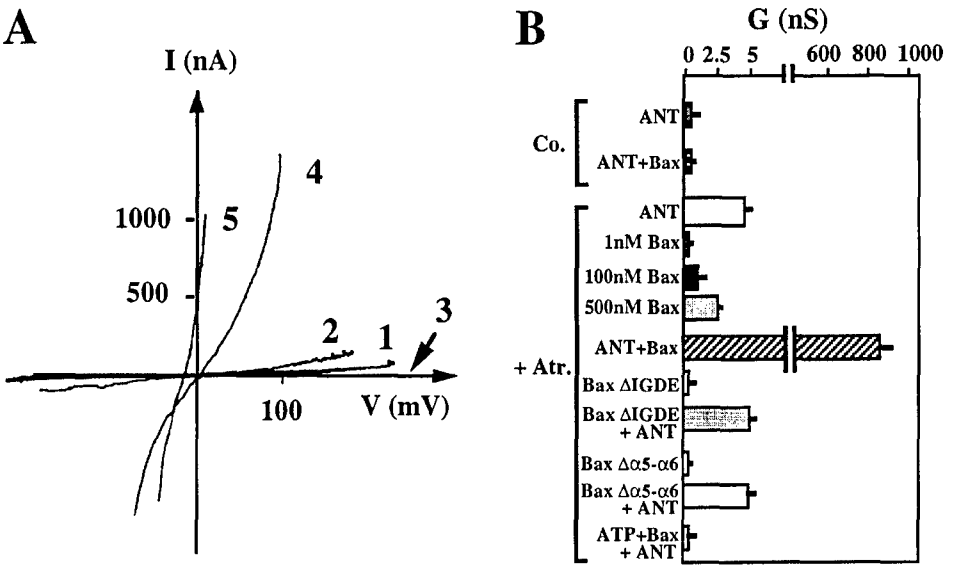

Figure 5 Macroscopic determination of the ANT-Bax cooperation. (**a**) Effects of Bax addition on macroscopic conductance of ANT. Current/voltage (I–V) curves were determined for preparations containing Bax only (1), Atr-treated ANT (2), ANT + Bax (3) or Atr-treated ANT + Bax (4, 5), in symmetric (1–4) or asymmetric (5) conditions. (**b**) Conductances determined from I–V curves in symmetric conditions. The conductance (corresponding to the slope of the I–V curve obtained in **c**) was calculated for different preparations of ANT (4 nM), in the presence of Bax (1 nM unless specified), mutated Bax proteins (1 nM BaxΔIGDE or BaxΔα5/6), ATP (1 mM) and/or Atr (40 μM), as indicated. These experiments have been repeated two to five times, yielding similar results

domain (G145A), which yields a channel with a reduced conductance (Figure 6b). Intriguingly, we found that, in combination with ANT, Bcl-2 does not form channels in artificial membranes (nor does Bcl-2 G145A), suggesting that the physical interaction between ANT and Bcl-2 (Marzo *et al.*, 1998a) can change the ion channel properties of Bcl-2. This effect is optimal in conditions of molar equivalence of ANT and Bcl-2. It becomes particularly evident when macroscopic measurements are performed (Figure 6c). The combination of ANT plus Bcl-2 results in a virtual cessation of ion movement indicative of the closure of both ANT and Bcl-2 channels. Though not shown, the channel activity of Bcl-2 was not influenced by Atr. If Bcl-2 is replaced by a mutant protein (Bcl-2 Δα5/6) lacking a putative pore formation domain (Matsuyama *et al.*, 1998; Schendel *et al.*, 1997), the inhibition of ANT-mediated conductance is suboptimal, both at the macroscopic (Figure 6c) and single channel levels (Figure 6a). In conclusion, Bcl-2 and ANT exhibit mutual inhibition of ion channel formation *in vitro*.

As expected (Antonsson *et al.*, 1997; Oltvai and Korsmeyer, 1994), an excess of Bcl-2 prevented the formation of channels induced by the combination of Bax and ANT (Figure 6d). Thus, in addition to its Bax-independent effect on the ANT (Figure 6a,b), Bcl-2 can neutralize Bax (Antonsson *et al.*, 1997; Oltvai and Korsmeyer, 1994), including the cooperative effect of Bax on ANT.

Concluding remarks

The electrophysiological data contained in this work reveal a close functional interaction between ANT and Bax, as well as between ANT and Bcl-2. Although each of these molecules can form ion channels, their combination has new, unexpected properties. Bax potentiates the capacity of ANT to form an Atr-responsive channel, whereas the combination of Bcl-2 and ANT is inactive. These observations may resolve the long-standing contradiction between Bcl-2 effects on synthetic membranes and on mitochondria. In artificial lipid bilayers, Bcl-2/Bcl-X_L forms a mostly cation-specific ion channel (Minn *et al.*, 1997; Schendel *et al.*, 1997; Schlesinger *et al.*, 1997). However, in isolated mitochondria or intact cells, Bcl-2/Bcl-X_L prevents the influx of water into the mitochondrial matrix and the dissipation of the $\Delta\Psi_m$ (Kroemer, 1997; Marzo *et al.*, 1998a,b; Narita *et al.*, 1998; Shimizu *et al.*, 1998; vander Heiden *et al.*, 1997; Zamzami *et al.*, 1996). As shown here, it becomes plausible that, within its physiological context (that is in the presence of other proteins including ANT), Bcl-2 acquires electrophysiological properties that have not been revealed in a more artificial setting. As a word of caution, it has to be stated, however, that the electrophysiological experiments in which ANT was reconstituted into the same synthetic lipid bilayer as Bax and Bcl-2 might inaccurately reflect the *in vivo* physiology of mitochondria, in which ANT is confined to the inner membrane whereas Bax and Bcl-2 are enriched in the outer membrane, within the contact site between inner and outer membranes (Krajewski *et al.*, 1993). At present, it remains unclear to which extent the interactions *in situ* involve close interactions between ANT and Bcl-2-like proteins (as they are suggested by co-immunoprecipitation studies

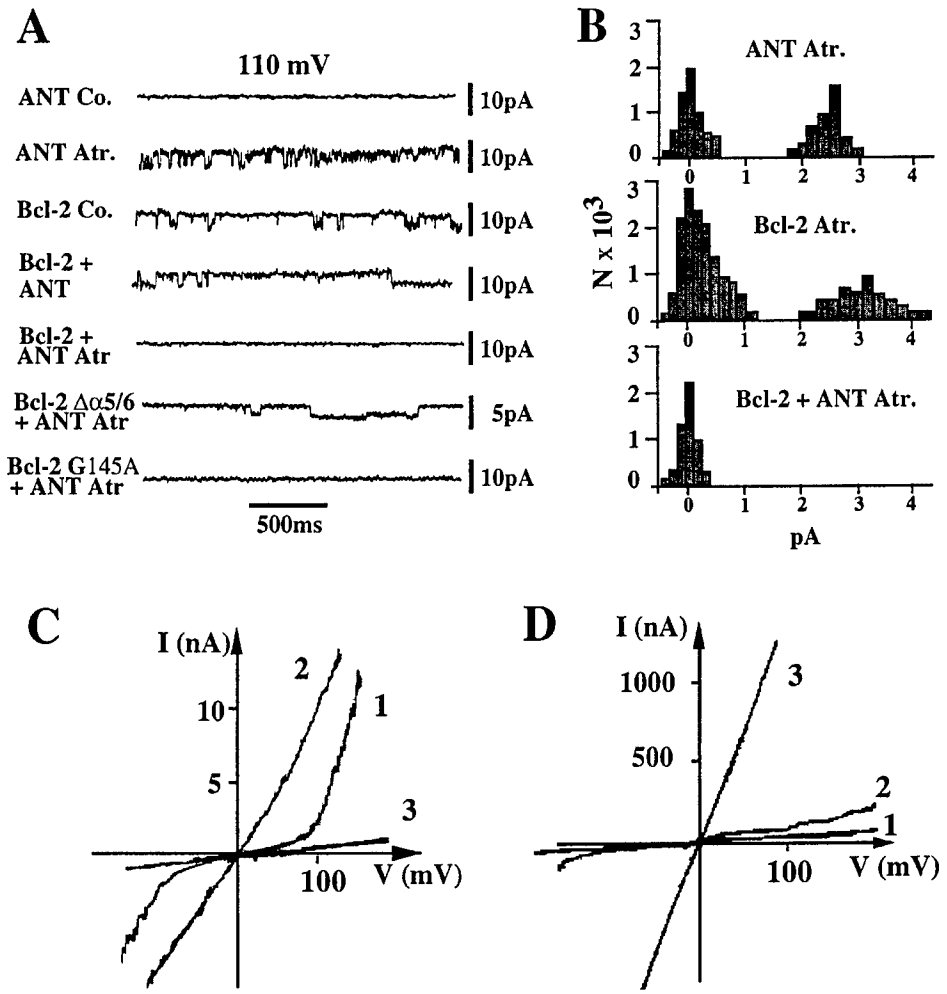

Figure 6 Electrophysiology of the ANT/Bcl-2 interaction. (**a**) Bcl-2 inhibits opening of the Atr/ANT channel at the single channel level. Recordings of single-channels of different combinations of ANT, Bcl-2 (molar ratio ANT : Bcl-2 = 1 : 1), Bcl-2 Δα5-α6, Bcl2 G145A and/or Atr obtained at a voltage of 110 mV. (**b**) Statistical analysis of channel opening and conductances obtained for Bcl-2 and Bcl-2 G145A. (**c**) Effects of Bcl-2 addition on macroscopic conductance of ANT. I–V curves were obtained in different conditions, namely in the presence of (Atr-treated) ANT (line 1), Bcl-2 alone (line 2) or an equimolar combination of both (line 3). All recordings were done in equimolar conditions (1 : 1; 20 nM). Note that the scale of the ordinate is different from Figure 2c. (**d**) Effect of Bcl-2 on the Bax/ANT cooperative effect. I–V curves were obtained with (Atr-treated) ANT (line 1), or ANT + BAX + Bcl-2 (10 : 1 : 10 molar ratio; line 2), or ANT + Bax (10 : 1; line 3), the amount of ANT being constant in each preparation. Experiments are representative of two to four independent data sets

(Marzo *et al.*, 1998a)) and/or a translocation of Bcl-2/Bax from the outer to the inner membrane.

Although the exact stoichiometry of the ANT/Bax or ANT/Bcl-2 reaction (e.g. heterodimers, heterotetramers or higher-order structures) remains elusive, the present data, as well as the earlier observations of direct physical Bcl-2/Bax (Oltvai *et al.*, 1993), ANT/Bax and ANT/Bcl-2 interactions (Marzo *et al.*, 1998a) may be integrated into a *ménage à trois* model of promiscuous interactions between ANT, Bax, and Bcl-2 within the PTPC. Hypothetically, one of the functions of Bcl-2 would be to withhold Bax from its functionally relevant site of action, which is the inner mitochondrial membrane, to which some Bax molecules may translocate in a colicin-like fashion (Marzo *et al.*, 1998a). An additional, Bax-independent function of Bcl-2 would be to interact with ANT, the core protein of the PTPC, and to prevent it from forming a pore. This Bax-independent function of Bcl-2 might be restricted to those ANT molecules interacting with the outer mitochondrial membrane within the contact site. In contrast, the major function of Bax, apart from neutralizing Bcl-2, would be to interact with ANT to facilitate pore formation in an ANT conformation-dependent fashion, thus allowing for ion and subsequent water influx into the matrix and final $\Delta\Psi_m$ dissipation. This scenario of 'apostat' regulation would be compatible with the reported autonomous, Bax-independent function of Bcl-2 and vice versa (Knudson and Korsmeyer, 1997). If correct, the *ménage à trois* model of ANT/Bcl-2/Bax interactions could have far-

reaching consequences for the development of new classes of apoptosis-inhibitory and apoptosis-inducing agents which selectively inhibit ANT/Bax and ANT/Bcl-2 interactions, respectively.

Materials and methods

Cell culture and microinjection

Rat-1 fibroblast cells transfected with a control vector only, Bcl-2 wild-type or Bcl-2 fusion proteins selectively directed to the mitochondrion (actA-Bcl-2) or the endoplasmic reticulum and nuclear envelope (cb5-Bcl-2) (Zhu *et al.*, 1996), were microinjected (pressure 150 hPa; 0.2 s; (Marzo *et al.*, 1998a)) with buffer only, atractyloside (50 μM) or horse cytochrome *c* (10 μM, Sigma). After microinjection, cells were cultured for 120 min and stained for 10 min with the $\Delta\Psi_m$-sensitive dye CMXRos and the DNA-intercalating dye Hoechst 33342, as described (Marzo *et al.*, 1998a). Microinjected viable cells (100–200 per session, two to three independent sessions of injection) were identified by inclusion of 0.25% (w:v) FITC-dextran (green fluorescence) in the injectate. Only the blue or red fluorescence was recorded.

Functional assays on purified and reconstituted PTPC in liposomes

PTPC from Wistar rat brains were purified and reconstituted in liposomes following published protocols (Marzo *et al.*, 1998b). Briefly, membrane-associated, Triton X-100-soluble proteins co-purifying with hexokinase 1 were enriched by anion exchange chromatography. Immunodepletion of ANT was performed at this stage using a polyclonal rabbit antibody (gift from Dr Heide H Schmid; (Giron-Calle and Schmid, 1996)). One volume of PTPC-containing preparation was incubated with one volume of polyclonal anti-ANT or an equivalent concentration of pre-immune rabbit antiserum for 2 h at 4°C. 0.1 volume of protein A and protein G agarose beads was added and the mix was incubated for 30 min at room temperature. The beads were collected by centrifugation (10 min, 2000 *g*), and the supernatant was used for further experiments. The PTPC (approx. 1 μg protein/mg lipid) were reconstituted into phosphatidylcholine/cholesterol (5:1=w:w) vesicles by overnight dialysis. Liposomes recovered from dialysis were ultrasonicated (120 W, Ultrasonic Processor, Bioblock) for 7 s in 5 mM malate and 10 mM KCl, charged on a Sephadex G50 column and eluted with 125 mM sucrose + 10 mM HEPES (pH 7.4). Proteoliposomes containing maximum hexokinase activity were recovered, as described (Marzo *et al.*, 1998b) and were incubated at room temperature for 30 min with different PT pore-opening agents in 125 mM sucrose + 10 mM HEPES (pH 7.4). For determination of 3,3'dihexylocarbocyanine iodide ($DiOC_6(3)$) retention, liposomes were equilibrated for 30 min with 80 nM ($DiOC_6(3)$) and then analysed in a cytofluorometer (Marzo *et al.*, 1998b).

Purification of ANT and recombinant Bax/Bcl-2 proteins

ANT was purified (Rück *et al.*, 1998) from rat heart mitochondria isolated as described (Susin *et al.*, 1999a). Mitochondria were subjected to mechanical shearing in a Emvejhem potter; solubilized (8 min, 4°C) in buffer A (220 mM mannitol, 70 mM sucrose, 10 mM HEPES (pH 7.4), 200 μM EDTA, 1 mM β-mercaptoethanol) supplemented with 0.5 mg/ml subtilisin; and subjected to differential centrifugation (5 min 500 *g*, discard pellet; then 10 min 10 000 *g*, discard supernatant). Soluble (30 min, 24 000 *g*, 4°C) mitochondrial proteins (10 mg/ml) were resuspended in buffer B (40 mM KH_2PO_4 (pH 6.0), 40 mM KCl, 2 mM EDTA, and 6% [vol:vol] Triton X100; Boehringer Mannheim, Mannheim, Germany). 2 ml of this solution were applied to a column containing 1 g hydroxyapatite (BioGel HTP, Biorad) and eluted with buffer B, then diluted 1:1 with buffer C (20 mM MES, 200 μM EDTA, pH 6.0; 0.5% Triton X-100) supplemented with 1 M NaCl, applied to a HiTrap SP column (Pharmacia Biotech, Uppsala, Sweden) pre-equilibrated with buffer C, washed with buffer C, and eluted at a flow of 1 ml/min by gradually increasing the salt concentration (0 to 500 mM NaCl within 10 min). ANT containing fractions were checked for purity using silver staining and immunoblot (12.5% SDS–PAGE, 3 μg protein/lane) using a monoclonal antibody recognizing VDAC (31HL, Calbiochem), a polyclonal rabbit antisera specific for ANT (see above), an antiserum raised against the N-terminus of cyclophilin D (gift from Paolo Bernardi, University of Padova, Padova, Italy; (Nicolli *et al.*, 1996)), Bcl-2 (specific for residues 20-34; Calbiochem, La Jolla, CA, USA), or Bax (Santa Cruz Biotechnology, Santa Cruz, CA, USA). Positive controls were total mitochondrial proteins (50 μg/lane) from the rat heart. Recombinant human Bcl-2 (1-218), mutant Bcl-2(Gly145Ala) and Bcl-2$\Delta\alpha$5/6 (Bcl-2 (Δ143-184), Bcl-2$\Delta\alpha$5/6 (Bcl-2 Δ143-184), murine Bax (1-171) or mutant Bax ΔIGDE (Δ66-69) and a Bax $\Delta\alpha$5/6 (Δ106-153) lacking the hydrophobic transmembrane domain (Δ219-239 in the case of Bcl-2; Δ172-192 for Bax) were purified as described (Jürgensmeier *et al.*, 1998; Schendel *et al.*, 1998; Xie *et al.*, 1998). Circular dichroism spectra revealed correct folding of all recombinant proteins.

Electrophysiological methods

The pore-forming activities of ANT, Bax, Bax ΔIGDE, Bax $\Delta\alpha$5/6, Bcl-2 and/or Bcl-2 $\Delta\alpha$5/6 were investigated at both the macroscopic (black membrane) and single-channel (patch clamp) levels, following published protocols (Brullemans *et al.*, 1994). The lipid mixture palmitoyloleoylphosphocholine/dioleoylphosphocholine (7:3; w:w) supplemented with 3% cardiolipin (Avanti Polar Lipids Inc., Alabaster, AL, USA) was dissolved in 1 or 0.1%. For the macroscopic conductance configuration, solvent free bilayers were formed by apposition of two lipid monolayers onto a 175–200 μm diameter hole in a 25-μm thick PTFE film sandwiched between two glass half cells pretreated with hexane/hexadecane (40:1 v/v) (Montal and Mueller, 1972). Unless specified, recordings were performed in symmetric conditions (100 mM KCl, 2 mM $MgCl_2$, 10 mM HEPES, pH 7.4). To determine anion/cation specificity, asymmetric conditions (400/100 mM KCl, cis/trans) were imposed on the bilayer and the reversal potential (V_{rev}) was calculated by means of the Goldmann-Hodgkin-Katz equation (Hille, 1984). For recording single-channel fluctuations, lipid bilayers were preformed at the tip of patch-clamp glass micropipettes by the 'tip-dip' method (Hanke *et al.*, 1984). Bilayer formation was monitored by the capacitance response and, prior to protein addition, bare membranes were checked under applied potentials for electrical silence. Before addition to the bilayer, proteins were incubated with 1 mM $CaCl_2$, 40 μM Atr or control electrolyte (10 mM HEPES, 100 mM KCl, 2 mM $MgCl_2$, pH 7.4) for 30 min at room temperature, then mixed with evaporated lipid mixture (60 μg protein per mg lipid) and treated with Biobeads SM-2 (BioRad) to eliminate Triton X-100. The lipid protein mixture was added to both sides of the bilayer in the macroscopic configuration and to the bath in the tip-dip configuration (2.5 μg protein/ml). In some experiments, Bax was added directly to the aqueous subphase after bilayer formation. Macroscopic current-voltage curves were repeated at least three times, and the single channel recordings (digitally stored and subsequently analysed using Satori 3.01 software from Intracel Ltd, Royston, UK) are representative of the most frequently observed events.

Abbreviations

ANT, adenine nucleotide translocator; Atr, atractyloside; $\Delta\Psi_m$, mitochondrial transmembrane potential; PT, permeability transition; PTPC, permeability transition pore complex.

Acknowledgements

We are indebted to Dr Pat Schmid (The Hormel Institute, University of Minnesota, USA) and Professor Paolo Bernardi (University of Padova, Padova, Italy) for antisera. This work has been supported by grants from ANRS, ARC, FRM, INSERM, LNC, and the French Ministry for Science (to G Kroemer), GDR no. 790 (to H Duclohier), NIH grant AG 15393 (to JC Reed) and Région Haute Normandie (Ph.D. grant to H Cadiou). HLA Vieira receives a fellowship from the Fundação para a Ciência e a Tecnolgia PRAXIS XXI, Portugal.

References

Antonsson B, Conti F, Ciavatta A, Montessuit S, Lewis S, Martinou I, Bernasconi M, Bernard A, Mermod J-J, Mazzei G, Maundrell K, Gambale F, Sadoui R and Martinou J-C. (1997). *Science*, **277**, 370–376.

Brullemans M, Helluin O, Dugast J-Y, Molle G and Duclohier H. (1994). *Eur. Biophys. J.*, **23**, 39–49.

Brustovetsky N and Klingenberg M. (1996). *Biochemistry*, **35**, 8483–8488.

Crompton M, Virji S and Ward JM. (1998). *Eur. J. Biochem.*, **258**, 729–735.

Giron-Calle J and Schmid HH. (1996). *Biochemistry*, **35**, 15440–15446.

Green DR and Reed JC. (1998). *Science*, **281**, 1309–1312.

Hanke W, Methfessel C, Wilmsen U and Boheim G. (1984). *Bioelectrochem. Bioenerg.*, **12**, 329–339.

Hille B. (1984). Selective permeability versus independence. In: *Ionic channels of excitable membranes*. Sinauer Associates Inc., Sauerland, MA, pp. 226–248.

Jürgensmeier JM, Xie Z, Deveraux Q, Ellerby L, Bredesen D and Reed JC. (1998). *Proc. Natl. Acad. Sci. USA*, **95**, 4997–5002.

Knudson CM and Korsmeyer SJ. (1997). *Nat. Gen.*, **16**, 358–363.

Krajewski S, Krajeswka M, Shabaik A, Miyashita T, Wang HG and Reed JC. (1994). *Am. J. Pathol.*, **145**, 1323–1336.

Krajewski S, Tanaka S, Takayama S, Schibler MJ, Fenton W and Reed JC. (1993). *Cancer Res.*, **53**, 4701–4714.

Kroemer G. (1997). *Nature Medicine*, **3**, 614–620.

Kroemer G, Dallaporta B and Resche-Rigon M. (1998). *Annu. Rev. Physiol.*, **60**, 619–642.

Liu XS, Kim CN, Yang J, Jemmerson R and Wang X. (1996). *Cell*, **86**, 147–157.

Mancini M, Nicholson DW, Roy S, Thornberry NA, Peterson EP, Casciola-Rosen LA and Rosen A. (1998). *J. Cell Biol.*, **140**, 1485–1495.

Marzo I, Brenner C, Zamzami N, Jürgensmeier J, Susin SA, Vieira HLA, Prévost M-C, Xie Z, Mutsiyama S, Reed JC and Kroemer G. (1998a). *Science*, **281**, 2027–2031.

Marzo I, Brenner C, Zamzami N, Susin SA, Beutner G, Brdiczka D, Rémy R, Xie Z-H, Reed JC and Kroemer G. (1998b). *J. Exp. Med.*, **187**, 1261–1271.

Matsuyama S, Schendel SL, Xie Z and Reed JC. (1998). *J. Biol. Chem.*, **273**, 30995–31001.

Minn AJ, Vélez P, Schendel SL, Liang H, Muchmore SW, Fesik SW, Fill M and Thompson CB. (1997). *Nature*, **385**, 353–357.

Montal M and Mueller P. (1972). *Proc. Natl. Acad. Sci. USA*, **69**, 3561–3566.

Narita M, Shimizu S, Ito T, Chittenden T, Lutz RJ, Matsuda H and Tsujimoto Y. (1998). *Proc. Natl. Acad. Sci. USA*, **95**, 14681–14686.

Nicolli A, Basso E, Petronilli V, Wenger RM and Bernardi P. (1996). *J. Biol. Chem.*, **271**, 2185–2192.

Oltvai ZN and Korsmeyer SJ. (1994). *Cell*, **79**, 189–192.

Oltvai, ZN, Milliman CL and Korsmeyer SJ. (1993). *Cell*, **74**, 609–619.

Rück A, Dolder M, Wallimann T and Brdiczka D. (1998). *FEBS Lett.*, **426**, 97–101.

Schendel S, Montal M and Reed JC. (1998). *Cell Death Differ.*, **5**, 372–380.

Schendel S, Xie Z, Montal MO, Matsuyama S, Montal M and Reed JC. (1997). *Proc. Natl. Acad. Sci. USA*, **94**, 5113–5118.

Schlesinger PH, Gross A, Yin XM, Yamamoto K, Saito M, Waksman G and Korsmeyer SJ. (1997). *Proc. Natl. Acad. Sci. USA*, **94**, 11357–11362.

Shimizu S, Eguchi Y, Kamiike W, Funahashi Y, Mignon A, Lacronique V, Matsuda H and Tsujimoto Y. (1998). *Proc. Natl. Acad. Sci. USA*, **95**, 1455–1459.

Susin SA, Larochette N, Geuskens M and Kroemer G. (1999a). *Meth. Enzymol.*, in press.

Susin SA, Lorenzo HK, Zamzami N, Marzo I, Larochette N, Alzari PM and Kroemer G. (1999b). *J. Exp. Med.*, **189**, 381–394.

Susin SA, Lorenzo HK, Zamzami N, Marzo I, Snow BE, Brothers GM, Mangion J, Jacotot E, Costantini P, Loeffler M, Larochette N, Goodlett DR, Aebersold R, Siderovski DP, Penninger JM and Kroemer G. (1999c). *Nature*, **397**, 441–446.

Susin SA, Zamzami N, Castedo M, Hirsch T, Marchetti P, Macho A, Daugas E, Geuskens M and Kroemer G. (1996). *J. Exp. Med.*, **184**, 1331–1342.

vander Heiden MG, Chandal NS, Williamson EK, Schumacker PT and Thompson CB. (1997). *Cell*, **91**, 627–637.

Woodfield K, Ruck A, Brdiczka D and Halestrap AP. (1998). *Biochem. J.*, **336**, 287–290.

Xie ZH, Schendel S, Matsuyama S and Reed JC. (1998). *Biochemistry*, **37**, 6410–6418.

Ying XM, Oltvai ZN and Korsmeyer SJ. (1994). *Nature*, **369**, 321–323.

Zamzami N, Susin SA, Marchetti P, Hirsch T, Gómez-Monterrey I, Castedo M and Kroemer G. (1996). *J. Exp. Med.*, **183**, 1533–1544.

Zhu W, Cowie A, Wasfy GW, Penn LZ, Leber B and Andrews DW. (1996). *EMBO J.*, **15**, 4130–4141.

DEPARTMENT OF THE ARMY
US ARMY MEDICAL RESEARCH AND MATERIEL COMMAND
504 SCOTT STREET
FORT DETRICK, MARYLAND 21702-5012

REPLY TO
ATTENTION OF

MCMR-RMI-S (70-1y) 8 Jan 2003

MEMORANDUM FOR Administrator, Defense Technical Information Center (DTIC-OCA), 8725 John J. Kingman Road, Fort Belvoir, VA 22060-6218

SUBJECT: Request Change in Distribution Statement

1. The U.S. Army Medical Research and Materiel Command has reexamined the need for the limitation assigned to the enclosed. Request the limited distribution statement for the enclosed be changed to "Approved for public release; distribution unlimited." These reports should be released to the National Technical Information Service.

2. Point of contact for this request is Ms. Judy Pawlus at DSN 343-7322 or by e-mail at judy.pawlus@det.amedd.army.mil.

FOR THE COMMANDER:

Encl

PHYLIS M. RINEHART
Deputy Chief of Staff for
Information Management

ADB265840	ADB266633	ADB282069
ADB279138	ADB251763	ADB265386
ADB264578	ADB281601	ADB282057
ADB281679	ADB258874	ADB258251
ADB281645	ADB281773	ADB264541
ADB261128	ADB281660	ADB241630
ADB261339	ADB259064	ADB281924
ADB273096	ADB266141	ADB281663
ADB281681	ADB281664	ADB281659
ADB259637	ADB258830	
ADB256645	ADB266029	
ADB262441	ADB281668	
ADB281674	ADB259834	
ADB281771	ADB266075	
ADB281612	ADB281661	